



ZAVARIVANJE I ZAVARENE KONSTRUKCIJE

WELDING & WELDED STRUCTURES

God. 64 Vol. 64	Br. 2 No. 2	49-96 49-96	Beograd Belgrade	Srbija Serbia	2019. 2019.
--------------------	----------------	----------------	---------------------	------------------	----------------

ČASOPIS DRUŠTVA ZA UNAPREĐIVANJE
ZAVARIVANJA U SRBIJI

SERBIAN WELDING SOCIETY
QUARTERLY REVIEW

IZLAZI TROMESEČNO

IZDAVAČ / PUBLISHER

**DUZS - Društvo za unapređivanje
zavarivanja u Srbiji**

Adresa: 11000 Beograd, Grčića Milenka 67

Za izdavača / For Publisher

Branislav Lukić, dipl.ing, predsednik DUZS

UREDNIŠTVO / EDITORIAL

Glavni i odgovorni urednik / Editor-in-Chief

Milica Antić, dipl.ing. EWE

duzs011@gmail.com, milicamantic@yahoo.com

Tehnički urednik / Technical Editor

Branislav Lukić, dipl.ing

Redakcijski odbor / Editorial Board

Dr Nenad Radović, dipl.ing.

Dr Radomir Jovičić, dipl.ing.

Dr Bore Jegdić, dipl.ing.

Miloš Pavlović, dipl.ing.

REDAKCIJA I MARKETING / EDITORIAL OFFICE AND MARKETING

Vesna Jović

Grčića Milenka 67, I sprat
11000 Beograd

Tel / Fax + 381 (11) 2420-652
(10-16h)

duzs@eunet.rs

www.duzs.org.rs



UREĐIVAČKI ODBOR / PUBLISHING COUNCIL

Dr Vencislav Grabulov, dipl.ing, (predsednik)

Prof. dr Miroslav Đurđanović, dipl.ing.

Prof.dr Vukić Lazić, dipl.ing.

Doc.dr Ismar Hajro, dipl.ing. (BiH)

Prof.dr Darko Bajić, dipl.ing. (Crna Gora)

Prof. dr Aleksa Blagojević, dipl.ing. (BiH, Republika Srpska)

Prof. dr Sveto Cvetkovski, dipl.ing. (Makedonija)

Doc. dr Tomaž Vuherer, dipl.ing. (Slovenija)

Prof. dr Ivan Samardžić, dipl.ing. (Hrvatska)

Dr Horia Dascau, dipl.ing. (Rumunija)

CIP - Каталогизacija u publikaciji
Nародна библиотека Србије, Београд
621.791

ZAVARIVANJE i zavarene konstrukcije :
časopis Društva za unapređivanje zavarivanja
u Srbiji = Welding & Welded Structures :
Serbian Welding Society quarterly review /
glavni i odgovorni urednik = editor-in-chief Milica Antić. –
Vol. 41, no. 1 (1996)- . - Beograd :
Društvo za unapređivanje zavarivanja u Srbiji,
1996-. (Beograd : VIS studio).-29 cm

Tromesečno.

ISSN 0354-7965 = Zavarivanje i zavarene konstrukcije
COBISS.SR-ID 105396743

CENE I NARUDŽBINA ZA 2019.

Cena pojedinačnog broja 825,00 dinara

Godišnja pretplata 2500,00 dinara

Tekući račun: 325-9500600002588-46

PRICE AND ORDER

Annual subscription: EUR 100

Account No. RS35325960160000041546

OTPVRS22 (VOJVOĐANSKA BANKA AD)

IBAN RS35325960160000041546

ŠTAMPA / PRINTED

“VIS STUDIO” d.o.o.

Aleksinačkih rudara 35, Beograd

Tiraž: 400 kom.

SADRŽAJ

CONTENTS



NAUKA • ISTRAŽIVANJE • RAZVOJ

SCIENCE • RESEARCH • DEVELOPMENT

53

ANALYSIS OF THE INFLUENCE OF DIFFERENT TYPES OF COATINGS ON INCREASING THE WORKING LIFE OF CONSTRUCTIONAL ELEMENTS OF THE VENTILATION MILL AND REDUCING THE WEAR OF WORKING SURFACES

ANALIZA UTICAJA RAZLIČITIH VRSTA OBLOGA NA POVEĆANJE RADNOG VEKA KONSTRUKCIONIH ELEMENATA VENTILACIONOG MLINA I SMANJENJE TROŠENJA RADNIH POVRŠINA

Marko Ristić, Ivana Vasović, Vladimir Bošković, Christof Sommitsch, Jasmina Perišić



NAUKA • ISTRAŽIVANJE • RAZVOJ

SCIENCE • RESEARCH • DEVELOPMENT

69

GMA ROOT WELDING OF PEARLITIC RAILS USING MAGNETIC ARC DEFLECTION

GMA ZAVARIVANJE KORENA PERLITNIH ŠINA KORIŠĆENJEM SKRETANJA MAGNETNOG LUKA

L. Weingrill, M. Schwald, D. Frühstück, C. Faustmann, N. Enzinger



PRAKSA

PRACTICE

23

NEW HIGHLY PRODUCTIVE TECHNOLOGY OF COMBINED WELDING OF MAIN PIPELINES OF MAJOR DIAMETER

NOVE VISOKO PRODUKTIVNE TEHNOLOGIJE KOMBINOVANOG ZAVARIVANJA GLAVNIH CEVOVODA VELIKOG PREČNIKA

Vladimir Khomenko



OBRAZOVANJE

EDUCATION

83

FORMATION OF ULTRAFINE GRAINED STRUCTURE IN PLAIN CARBON STEELS THROUGH THERMOMECHANICAL PROCESSING

STVARANJE ULTRAFINOZRNE STRUKTURE KOD RAVNIH UGLJENIČNIH ČELIKA TERMOMEHANIČKOM OBRADOM

Hossein Beladi, Georgina L. Kelly and Peter D. Hodgson



VESTI

NEWS

52

REPUBLIČKO TAKMIČENJE MLADIH ZAVARIVAČA „MLADI ZAVARIVAČ 2019“

93

REPUBLIČKO TAKMIČENJE MLADIH ZAVARIVAČA „MLADI ZAVARIVAČ 2019“ -nastavak

96

MARKETING

Poštovani čitaoci,

Ono što je bio događaj od značaja je svakako takmičenje mladih zvarivača o čemu vam dajemo prikaz.

Nastavljamo sa prezentovanjem radova sa 4. IIW kongresa zavarivanja Jugoistočne Evrope. Iz tog opusa izdvajamo aktuelnu tematiku zavarivanja gasovoda velikih prečnika, onako kako se to radi u Rusiji.

Pored ovih, imaćete priliku da se ovoga puta upoznate i sa novim načinima zavarivanja šina, kroz rad izlagan u okviru međunarodne konferencije sa temom “Advanced Welding and Smart Fabrication Technologies for Efficient Manufacturing Processes” u okviru „The 71 IIW Annual Assembly & International Conference“, July 2018 | Bali, Indonesia.

To naravno nije sve, možete još pročitati i jedan interesantan rad vezan za čelike kod kojih se jako finostruktura postiže termomehaničkom obradom.

Do narednog susreta

***Glavni i odgovorni urednik
Milica Antić, dipl.ing, EWE***



Republičko takmičenje mladih zavarivača „Mladi zavarivač 2019“, Novi Sad, 10-11. Maj 2019

U petak i subotu, 10-11. maja u okviru proizvodnog pogona “Pobeda” u Petrovaradinu održano je republičko takmičenje „Mladi zavarivač 2019.“

Organizatori takmičenja bili su: Ministarstvo prosvete, nauke i tehnološkog razvoja RS, Zajednica mašinskih škola Republike Srbije (ZMŠ RS), Srednja mašinska škola Novi Sad i Društvo za unapređivanje zavarivanja u Srbiji (DUZS).

Takmičenje mladih zavarivača u Srbiji organizovano je, u tri postupka zavarivanja (111-REL; 135-MAG; 141-TIG).

Prijavljeno je 39 takmičara iz 16 srednjih mašinskih škola: Tehnička škola „Kolubara“ Lazarevac, Tehnička škola Obrenovac, Tehnička škola Železnik, Tehnička škola Čuprija, Tehnička škola Odžaci, Tehnička škola Kosovska Kamenica, Tehnička škola Vlasotince, Prva tehnička škola Kruševac, Mašinska škola Niš, Srednja škola Krupanj, Srednja mašinska škola Novi Sad, Srednja stručna škola Kragujevac, Tehnička škola sa domom učenika “Nikola Tesla” Kostolac, Srednja tehnička škola “Milenko Brzak Uča” Ruma, Tehnička škola “Ivan sarić” Subotica, Srednja škola “17.septembar” Lajkovac.



Na otvaranju takmičenja učesnike je pozdravio Gavranić Vladimir, direktor srednje mašinske škole Novi Sad



Priprema učesnika za praktičan deo

Nastavak na strani 93.



Marko Ristić^{1,a}, Ivana Vasović^{1,b}, Vladimir Bošković^{1,c}, Christof Sommitsch^{2,c}, Jasmina Perišić^{1,d}

Analysis of the influence of different types of coatings on increasing the working life of constructional elements of the ventilation mill and reducing the wear of working surfaces

Analiza uticaja različitih vrsta obloga na povećanje radnog veka konstrukcionih elemenata ventilacionog mlina i smanjenje trošenja radnih površina

Originalni naučni rad / Original scientific paper

Rad je u izvornom obliku objavljen u Zborniku sa 4. IIV Kongresa zavarivanja Jugoistočne Evrope „Safe Welded Construction by High Quality Welding“ održanog u Beogradu 10-13. Oktobra 2018

Rad primljen / Paper received:

April 2019.

Ključne reči: ventilacioni mlin, trošenje, prevlake-obloge, višefazni tok, nanošenje, radni vek

Rezime

U radu su analizirane mogućnosti povećanja otpornosti na habanje delova ventilacionog mlina za mlevenje uglja u elektranama, analizom sa multidisciplinarnim istraživanjima. Delovi ventilacionog mlina izloženi su veoma složenim radnim uslovima (velika brzina čestica, prisustvo peska do 40% i druge mineralne komponente). Upotrebom CFD 3D numeričke simulacije višefaznog toka u mlinu, analizirana je brzina, koncentracija i ugao protoka smese oko radnih delova. Analizirajući potencijalnu primenu obloga otpornih na habanje na radnim delovima ventilacionog mlina, ima za cilj da poveća preostali radni vek radnih elemenata. Analizirajući oštećene delove ventilacionog mlina i koristeći numeričku simulaciju oko radnih elemenata, odabrana je široka paleta dodatnih materijala otpornih na habanje za eksperimentalna ispitivanja. Za analizu mogućnosti poboljšanja svojstava površine, obloge otporne na habanje nanose se različitim tehnikama: ručnim elektrolučnim zavarivanjem, HVOF talozima i plazma zavarivanjem, a koriste se i dodatni materijali različitih hemijskih sastava. Struktura uzoraka se analizira sa SEM-EDS i merenjem i distribucijom tvrdoće u presecima uzoraka. Verifikacija analiziranog rezultata vrši se eksperimentalnim ispitivanjem, sprovođenjem simulacije trošenja u ventilacionom mlinu na uzorcima u komori mašina za peskarenje. Medijum za simulaciju habanja je kvarcni pesak i uzorci su postavljeni pod uglom od 20°. Primena ovog istraživanja može povećati radni vek delova u termoenergetskim objektima, smanjiti broj mogućih

Adresa autora / Author's address:

^a Institute Mihailo Pupin, Volgina 15 Belgrade, Serbia

^b Lola Institute, Kneza Višeslava 70a, Belgrade, Serbia

^c Institute of Materials Science, Joining and Forming, Kopernikusgasse 24/I 8010 Graz, Austria,

^d Union - Nikola Tesla University, Cara Dušana 62-64, Belgrade, Serbia

Key words: ventilation mill, wear, coatings, multiphase flow, depositions, working life

Abstract

Research presented in this paper analyzed the possibilities of increasing the wear resistance of the ventilation mill parts for coal grinding in power plants, analyzing with multidisciplinary research. The parts of ventilation mill are exposed in very complex working condition (high velocity of particles, presence of sand up to 40% and other mineral components). Using the CFD 3D numerical simulation of multiphase flow in grinding mill, is analyzed the speed, concentration and flow angle of mixture around working parts. Analyzing the potential application of wear resistance coating on the working parts ventilation mill have goal to increase remaining working life of working elements. By analyzing the damaged parts of ventilation mill and using the numerical simulation around working elements, are selected wide pallet of wear resistance filler materials for experimental testing. To analyze possibilities to improve surface properties, the wear-resistant coatings were deposited by various technologies: manual metal arc welding, HVOF depositions and plasma welding and also are used filler materials with different chemical compositions. Samples structure is analyzed with SEM-EDS and also by measurement and distribution of hardness in the samples cross-sections. Verification of analyzed result is done by experimental testing, performing simulation of wear in ventilation mill on the samples in sandblasting machines chamber. Medium for simulating wear is quartz sand and the samples are positioned at angle 20°. Application of this research can increase working life of parts in thermoenergetic facilities, reduce the number of possible repairs and extends



popravki i produžiti period između njih. Time se postižu značajni ekonomski efekti.

Uvod

Nema sumnje da je energija oblast od posebnog značaja za čitavu privredu i društvo. Ako je proizvodnja energije stabilna kao moderan i dobro organizovan sektor, sigurno je da će to značiti dobro za celokupnu privredu zemlje. Nasuprot tome, ako se energiji ne posveti dovoljno pažnje sa stanovišta strateškog planiranja, postoji određena slaba pozicija i slabi izgledi privrede u celini [1]. Najverovatniji scenario globalnog razvoja pretpostavlja ekonomiju zasnovanu na efikasnoj upotrebi relativno "čistih" i iz različitih izvora, raspoložive energije. Prema svim razvojnim scenarijima postoji tendencija smanjenja energetske intenzivnosti ili potrošnje po jedinici novčanog proizvoda [1-3]. Glavni cilj ovog rada je da analizira mogućnost povećanja otpornosti na habanje delova ventilacionog mlina za mlevenje uglja u elektranama. Ovom analizom biće izabrana optimalna tehnologija za nanošenje prevlaka-obloga radnih delova koji su izloženi oštećenjima i habanju. Materijali i konstrukcije u rudarskim i energetskim industrijama oštećuju se pod uticajem brojnih faktora, kao što su: različita mehanička naprezanja, povišena-niska temperatura, sastav i atmosferski uslovi, oblici i dimenzije dela ili konstrukcije; struktura i svojstva materijala i kvaliteta površine [1,2]. Svi ti faktori pojedinačno utiču na radni vek materijala i konstrukcija, ali mnogo veći uticaj imaju u međusobnoj interakciji. Danas razvoj i projektovanje nije moguće bez korišćenja raznih 3D programa za modeliranje i za analizu struktura i ponašanja delova i konstrukcija. Optimizacija konstrukcije sa numeričkim analizama je dobro poznat pristup za poboljšanje performansi proizvoda koji se koriste u svim granama nauke i industrije [3, 4]. Pristup ovom radu je objedinjavanje multidisciplinarnih istraživanja ventilacionih mlinova termoelektrana, koji uključuju različite teorijske, numeričke, empirijske i eksperimentalne metode [5-8]. U dostupnoj literaturi prikazana je upotreba numeričkih metoda za različite aplikacije širom sveta, što dovodi do optimizacije kompleksnog sistema. [9]

Ovo istraživanje je nastavilo prethodna istraživanja koja su sprovedena za druge radne delove ventilacionog mlina. Udarne ploče ventilacionog mlina su već redizajnirane i potvrdile su da je numerička simulacija dobar alat za smanjenje broja modalnih eksperimenata i za precizniju analizu procesa koji se javljaju tokom kompleksnog toka koji mogu ukazati na potencijalnu metodologiju redizajna. [9]

the period between them. This achieves significant economic effects.

Introduction

There is no doubt that energy is a field of special importance for the entire economy and society. If energy producing is stable as modern and well-organized sector, it is certain that this will mean good for the entire economy of the country. Conversely, if energy is not given enough attention from the strategic planning point of view there is a certain weak position and weak prospects of the economy as a whole [1]. The most likely scenario of global development assumes an economy based on the efficient use of relatively "pure" and from various sources of available energy. According to all development scenarios have tendency of decreasing energy intensity or spending per unit of money product [1-3]. The main aim of this paper is, to analyses the possibility of increasing the wear resistance the parts of ventilation mill for coal grinding in power plants. By this analysis it will be selected optimal technology for coating of working parts which are exposed to damages and wear. Materials and construction in mining and energetic industries damages under the influence of numerous factors, such as: various mechanical stresses, elevated-low temperature, composition and atmospheric conditions, shapes and dimensions of a part or construction; structure and properties of material and quality of surface [1,2]. All those factors have individually effect on the working life of materials and constructions but much higher influence have in mutual interaction. Today development and designing is not possible without using various 3D programs for modeling and for analyses of structures and behavior of parts and constructions. Construction optimization with numerical analyses is a well-known approach for improving product performances which are used in all branches of science and industry [3, 4]. Approach of this paper is to unite multidisciplinary research of ventilation mills of thermal power plants includes a variety of theoretical, numerical, empirical and experimental methods [5-8]. The available literature shows the worldwide usage of numerical methods for different applications leading to optimization of the complex system. [9] This research has continued the previous research which conducted for other working parts of ventilation mill. Impact plates of ventilation mill is already redesigned and confirmed that numerical simulation is a good tool for reducing the number of modal experiments and for more precise analysis of process which occur during the complex flow which can indicate potential redesign methodology. [9]



CFD studija višefaznog toka pomoću Euler-Euler-ovog modela smeše predstavljena je u referencama [1, 2, 6, 8]. Višestruki protok smeše u ventilacionom postrojenju čine vazduh, uglj, pesak i druge mineralne čestice. Problem nosivosti radnih delova ventilacionog mlina javlja se tokom visokog prisustva peska u smeši, procenat peska zavisi od kvaliteta uglja i ne može se uticati na njega. Procenat peska u smeši može biti do 40% uglja. Zbog velike brzine čestica peska dolazi do izraženog trošenja elemenata brusnog točka i zidova mlina, smanjujući vremenski period između dve popravke i njihovog životnog veka.

U ovom radu analizirana je interakcija svih čestica sa površinom radnih delova ventilacionog mlina u dvofaznom sistemu gasu - čvrste čestice. Na ovaj način će se prikazati i analizirati strujanje oko kućice ventilacionog mlina oko elementa koji daje dodatno brušenje i postavlja se na kućicu mlina. Oštećenja se indirektno određuju na osnovu rezultata numeričke simulacije protoka; vektori brzine i raspodele čestica u kućnom ventilacionom mlinu. [1-3, 6-10].

Za povećanje radnog veka elementa u ventilacionom mlinu koristi se proces oblaganja. Koriste se originalni radni delovi i obloženi su samo materijalom koji ima otpornost na habanje. Oblaganje predstavlja pouzdanu metodu površinske obrade, koja je odabrana za poboljšanje površinskih svojstava materijala radnih delova, u kojem naneti materijal daje druge karakteristike originalnim radnim delovima. Za potrebe ovog istraživanja, upotrebljeni sloj koji ima odličnu otpornost na habanje i oksidaciju, homogeno se nanosi na površinu podloge [3-5, 11].

Analiza prethodnih eksperimentalnih istraživanja pokazala je linearnu zavisnost otpornosti na abrazivno trošenje i mehaničkih svojstava materijala. [8, 10-14] Na osnovu mehaničkih svojstava, posebno tvrdoće, može se predvideti ponašanje metala u uslovima habanja, ali tvrdoća nije jedina karakteristika koja utiče na otpornost na habanje i trošenje uopšte. Parametri, koji takođe utiču na otpornost na habanje, su struktura, oblik, veličina i raspored mikrokonstituenata u nanetom sloju [8-12].

Izbor optimalnih postupaka oblaganja, dodatnih materijala i tehnologije nanošenja vrši se na osnovu rezultata numeričkih simulacija, strukturnih i mehaničkih analiza uzoraka iz modela eksperimentalnog oblaganja.

Elementi prepreka u kućici ventilacionog mlina (položaj je prikazan strelicama na slici 1). Elementi prepreka se nalaze u kućici ventilacionog mlina između radnog točka i kućice ventilacionog mlina i

CFD study of the multiphase flow by using a Euler-Euler, mixture model is presented in references [1, 2, 6, 8]. Multiphase flow of mixture in ventilation mill consist form air, coal, sand and other mineral particles. Problem of wears working parts of ventilation mill occur during the high presence of sand in the mixture, percentage of sand depend form coal quality and cannot be influence on it. Percentage of sand in the mixture can be up to 40% of coal. Due to the high velocity of sand particles, pronounced wear of the grinding wheel elements and mill walls occurs, decreasing the time period between the two repairs and their lifespan.

The all particles interaction is analyzed with the surface of working parts of ventilation mill in a two-phase gas-solid particle flow are analyzed in this paper. In this appear it will have presented and analyzed flow around house of ventilation mill around the element which give additional grinding and positioned on house of mill. Damages are indirectly determined based on the results of the flow numerical simulation; vectors of the velocity and distribution of particles in the house ventilation mill. [1-3, 6-10].

For increasing the working life of element in ventilation mill is used coating process. It's used original working parts and only coated with material which have resistance to wear. Coating present reliable surface treatment method, which selected to improve the surface properties of working parts material, in which a coated material, give the others characteristic to original working parts. For the purpose of this research is a used coat that has excellent resistance to wear and oxidation, is homogeneously deposited onto the surface of a substrate [3-5, 11].

Analyzing the previous experimental research has indicated a linear dependence of abrasive wear resistance and mechanical properties of materials. [8, 10-14] Based on the mechanical properties, especially hardness, the behavior of metals in the conditions of wearing can be predicted, but hardness is not the only characteristic that affects the wear resistance and wear in general. Parameters, which also affect the wear resistance, are the structure, shape, size and distribution of microconstituents in the coating [8-12].

The selection of optimal coating procedures, filler materials and coating technology is done based on the results of numerical simulation, structural and mechanical analyses of samples from experimental coating model.

The obstacles elements in house of ventilation mill (position is shown by arrows Figure 1). Obstacles elements are located at the house of ventilation mill



mogu povećati efekat rešetke i generalno efikasnost ventilacionog mlina.

Elementi prepreka povećavaju finoću mlevenja ugljena, ali i smanjuju kapacitet ventilacionog mlina, stoga je potrebno ukloniti separator ugljene prašine iz mlina. Na taj način, proces protoka mlevenog uglja u ventilacionom mlinu sa elementima prepreka, značajno smanjuje trošenje radnih elemenata mlina, a posebno radnih kola sa udarnim pločama, produžava radno vreme ovih mlinova i poboljšava proces sušenja ugljene prašine.

Prethodna istraživanja ukazuju da povećanje broja prepreka povećava broj mogućih sudara čestica ugljene prašine i na taj način povećava efikasnost brušenja. Takođe, na efikasnost brušenja može uticati povećanje dimenzija prepreka kao i smanjenje rastojanja između radnog točka i kućice ventilacionog mlina (smanjujući prosečni prečnik položaja prepreka).

Primer uspešne rekonstrukcije kombinovanog ventilacionog mlina DGS 100S, koji se nalazi u TE Nikola Tesla A u Obrenovcu, detaljno je opisan u literaturi. [3, 4, 14] Cilj rekonstrukcije je postizanje povećanog mlevenja uglja. Ploče su postavljene u spiralu kućice ventilacionog mlina kao prepreka na izlazu iz mlina do područja kanala za prašinu.

Dalji eksperiment je sproveden kako bi se povećao broj prepreka smeštenih u kućici ventilacionog mlina. Testovi su izvedeni sa 9, 10, 11, 12, 14, 15, 24 i 25 elementima prepreka. Postavljeni su u nizu sa udarnim točkom, počevši od izlaza ventilacionog mlina do kanala za prašinu, povećavajući njihov broj na jednu tačku gde svih 25 prepreka pokrivaju celu kućicu ventilacionog mlina

Za simulaciju procesa trošenja koriste se mašine za peskiranje. Verifikacija analiziranog rezultata vrši se eksperimentalnim ispitivanjem na uzorcima u komori mašine za peskiranje. Medijum za simulaciju habanja je kvarcni pesak i uzorci su postavljeni pod uglom od 20° .

1. Numerička simulacija i analiza rezultata modela smše

Numerička simulacija višefaznog toka u ovom istraživanju, predstavlja prvi korak u identifikaciji mogućnosti za revitalizaciju delova mlina izloženih habanju. Analizirajući vektor brzine i raspodelu protočnih mešavina, tj. čestice, moguće je locirati kritične tačke u konstrukciji ventilacionog mlina. Karakter višefaznog toka u ventilacionom mlinu TE-Kostolac B, u kome učestvuju komponente

between working wheel and house of ventilation mill and they can increase effect of gridding and generally the ventilation mill efficiency.

The obstacles elements increase the fineness of grinding of coal but it also reduces the ventilation capacity of the mill, therefore, it is necessary to remove the coal dust separator from the mill. In this way, the flow process of coal grinding in a ventilation mill with obstacles elements significantly reduces the wear of the working elements of the mill and especially the working wheel with impact plates extend working time of these mills and improves the process of coal dust drying.

Previous research indicates that increasing the number of obstacles elements increases the number of possible collisions of coal dust particles and in this way increases the efficiency of grinding. Also, the grinding efficiency can be influenced by increasing the dimensions of the obstacles as well as by reducing the distance between the working wheel and house of ventilation mill (reducing the average diameter of position of obstacles elements). An example of a successful reconstruction of the combined ventilation mill DGS 100S, which is located at the TE Nikola Tesla A in Obrenovac, is described in detail in the literature. [3, 4, 14] The goal of the reconstruction is to achieve an increase grinding of coal. The plates were placed in the spiral of the ventilation mill house as an obstacle at the exit from ventilation mill to area of dust channel. Further experiment was carried out in order to increase the number of obstacles placed in the house of ventilation mill. The tests were carried out with 9, 10, 11, 12, 14, 15, 24 and 25 obstacles elements. They were placed in a row with the impact wheel starting from the exit of ventilation mill to the dust channel, increasing their number to one point where whole 25 obstacles cover whole house of ventilation mill.

To simulate the process of wear is used sandblasting machines. Verification of analyzed result is done by experimental testing performed at the samples in sandblasting machines chamber. Medium for simulating wear is quartz sand and the samples are positioned at angle 20° .

1. Numerical simulation and analyses of results mixture model

The numerical simulation of the multiphase flow in this research present the first step in identifying possibilities for revitalization of the mill parts exposed to wear. By analyzing the velocity vector and the distribution of flow mixtures, i.e. particles, it is possible to locate the critical points in the construction of the ventilation mill. Character of multiphase flow in the ventilation mill TE-Kostolac



vazduha, ugljene prašine, peska i drugih minerala, direktno je povezan sa ranom funkcijom ventilacione efikasnosti mlina, kao i sa procesom habanja vitalnih delova. Promene u kvalitetu i protoku parametara mešavine direktno utiču na promene u komori za sagorevanje i kotlarnici. Programski paket ANSYS FLUENT zasnovan na metodi konačne zapremine koristi se za numeričke simulacije protoka.

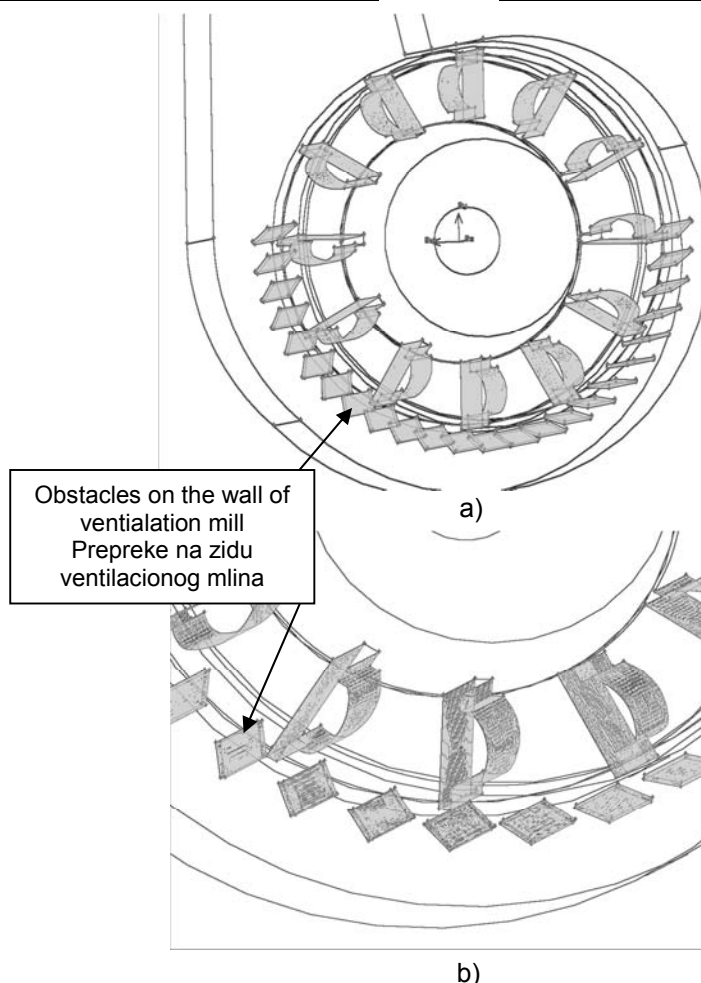
Reynoldsove prosečne Navier-Stokesove parcijalne diferencijalne jednačine turbulentnog višefaznog toka u mlinu rešene su. Dobijeno je rešenje disperzovanog gasa - čvrste struje, gde su granularne faze praškaste čestice lignita i peska. Vлага uglja se uvodi kao gasna faza [1-6]. Numerička simulacija višefaznog toka u ventilacionom mlinu sa preprekama prvi je korak u istraživanju uticaja prepreka na zidu mlina na karakteristike ventilacionog mlina i izbor geometrije prepreka. Za potrebe ovog istraživanja koristi se numerička simulacija za analizu protoka u ventilacionom mlinu, za dva modela i šest geometrija sa različitim položajem i uglom prepreke. Prepreke elementa mlina su predstavile ploče na zidu ventilacionog mlina koje imaju za cilj povećanje efekta rešetke. Lokacija ovih prepreka prikazana je na slici 1. Lagranžovski pristup (DPM) ubrizgava čestice čvrste faze i prati njihovo kretanje u gasnoj fazi. Prva generiše potrebnu geometriju, tj. oblik udarnih ploča i elemenata prepreka, kao i njihov položaj i međusobnu udaljenost. U drugom koraku, mreža se generiše u numeričkom domenu. Treći korak obuhvata izbor višefaznog modela, definisanje primarne i sekundarne faze, definisanje graničnih i početnih uslova, turbulentnog modela, numeričku simulaciju do konvergencije rešenja i analizu dobijenih rezultata.

Efikasnost brušenja u ventilacionom mlinu zavisi, pre svega od veličine kinetičke energije koja se prenosi na čestice uglja u njihovim sudarima sa udarnim elementima pokretača. U ventilacionim mlinovima, sudari se javljaju pretežno na ulaznoj ivici udarne ploče pri brzinama koje su približno jednake prosečnoj brzini ploče na tački kontakta čestica u rasponu od 50-60 m/s. Dalje mljevenje se odvija trenjem čestica na udarnoj površini kada se kreće prema izlaznom rubu ploče. Drobljene i sušene čestice uglja, koje su prošle kroz udarne ploče ventilacionog mlina, dosežu apsolutnu brzinu na izlazu od 80-100 m/s.

B, where components of air, coal dust, sand and other minerals particles participate, is directly related to the operation function of the ventilation efficiency of the mill, as well as to the wear process of vital parts. Changes in quality and flow of the mixture parameters directly affect changes in the combustion chamber and boiler plant. The ANSYS FLUENT software package based on the finite volume method is used for numerical flow simulations.

The Reynolds averaged Navier–Stokes partial differential equations of the turbulent multiphase flow in the mill are solved. A solution of the dispersed gas–solid flow is obtained, where granular phases are pulverized lignite and sand particles. The coal moisture is introduced as gas phase [1-6]. Numerical simulation of multiphase flow in a ventilation mill with obstacles is the first step in exploring the impact of obstacles on the wall of mill on the characteristics of the ventilation mill and the selection of the geometry of obstacles. For the purpose of this research numerical simulation is used to analyze flow in ventilation mill, for the two models and six geometries of with different position and angle of obstacles elements. Obstacles elements of mill have presented the plates on the wall of ventilation mill which have purpose to increase the effect of gridding. Location of these obstacles is shown on Figure 1. Lagrangian approach (DPM) injects solid phase particles and monitors their motion in the gaseous phase. The first generates the required geometry, that is, the shape of the impact plates and obstacles elements, as well as their position and mutual distance. In the second step, a network is generated in the numeric domain. The third step involves the choice of a multiphase model, the definition of primary and secondary phases, the definition of boundary and initial conditions, a turbulent model, numerical simulation to the convergence of the solution, and analyzes the obtained results.

The efficiency of grinding in ventilation mill depends primarily on the size of the kinetic energy that is passed on to coal particles in their collisions with impact elements of the impeller. In ventilation mills, collisions occur predominantly at the input edge of the impact plate at speeds approximately equal to the average velocity of the plate at the particle contact point in the range of 50-60 m/s. Further grinding takes place by friction of the particles on the impact surface when moving it towards the outlet edge of the plate. Crushed and dried coal particles, which passed through the impact plates of the ventilation mill, reach the absolute speed at an output of 80-100 m/s.



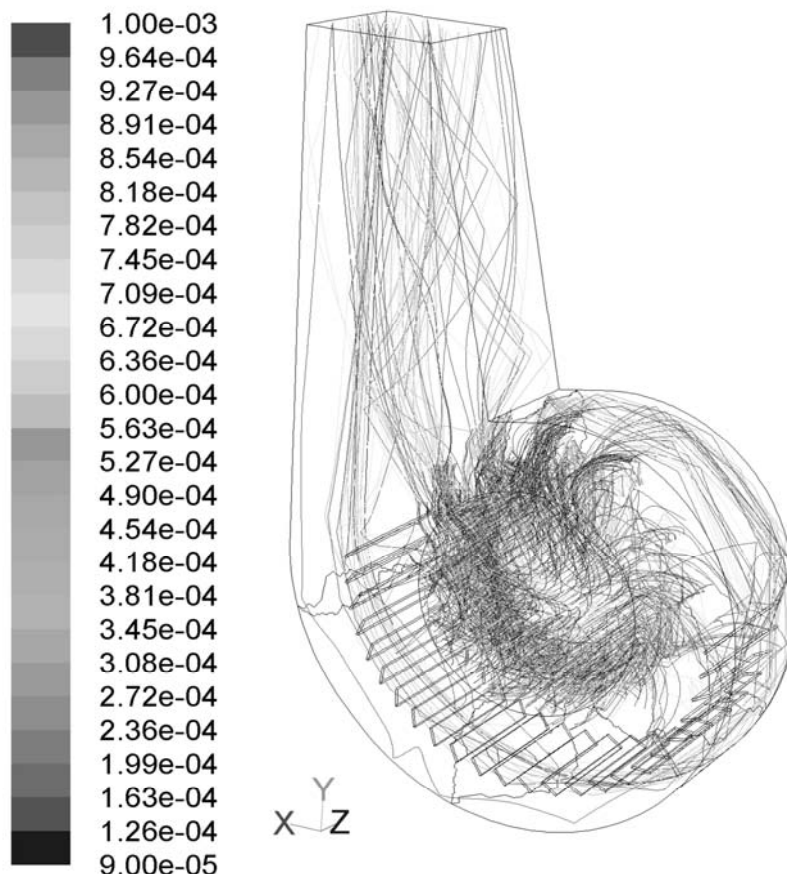
Slika 1. a) Geometrijski model ventilacionog mlina sa kanalom i komorama do ulaza u gorionik, b) Rotorsko kolo sa udarnim i usisnim pločama (strelice označavaju lokacije usisnih ploča)

Figure 1. a) The geometric model of the ventilation mill with duct and channels to the entrance at the burner, b) Impeller wheel with impact and suction plates (arrows indicates locations of suction plates)

Za DPM dodavanje uglja, korišćena je Rosin-Ramller-ova distribucija za četiri intervala prečnika: od 0 do 90 μm , od 90 do 200 μm , od 200 do 500 μm i od 500 do 1000 μm . Procentualno prisustvo za ova četiri intervala ispunjava zahtev da normalno oko 80% čestica praškastog uglja ima prečnik do 300 μm , tako da je srednji prečnik 152 μm i da parametar rasipanja ima vrednost 1.5227. Korišćene su tri veličine čestica: 300 μm , 800 μm i 1500 μm , pri čemu su čestice ubrizgane svakim od ova tri prečnika pojedinačno, a istovremeno ubrizgavanje čestica iz sva tri prečnika.

Na slici 2 prikazana je putanja čestice ugljene prašine za elemente prepreka pod uglom od 45° i centralnim uglom od 8° , a staze su obojene zavisno od prečnika čestica. Može se videti da povećanje veličine čestica povećava broj njihovih uticaja na elemente prepreka, dok manje čestice, zbog manje inercije, bliže prate protok gasne faze, ili se kreću duž obima mlina i imaju manje uglova odbacivanja u kanalu za prašinu.

For the DPM coal injection, Rosin-Ramller distribution was used for four intervals of diameter: from 0 to 90 μm , from 90 to 200 μm , from 200 to 500 μm and from 500 to 1000 μm . The percentage presence for these four intervals fulfills the requirement that normally about 80% of coal powder particles have a diameter of up to 300 μm , so that the mean diameter is 152 μm and the spreading parameter has a value of 1.5227. Three sand sizes of particles were used: 300 μm , 800 μm and 1500 μm , whereby particles were injected with each of these three diameters individually, and at the same time injection of particles from all three diameters. Figure 2 shows the path of coal dust particles for obstacles elements at an angle of 45° and a central angle of 8° , and the paths are colored by the particle diameter. It can be seen that increasing particle size increases the number of their impacts on obstacles elements, while smaller particles, due to less inertia, more closely monitor the flow of the gaseous phase, or move along the circumference of the mill and have fewer rejection angles in the dust channel.



Slika 3. Putanja čestica ugljenog praha do elementa prepreka postavljenih pod 45° i sa centralnim uglom od 8° , obojene putanje prečnika čestica

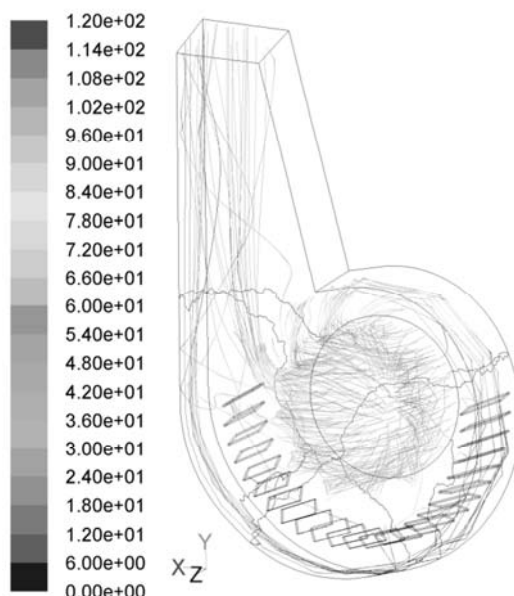
Figure 3. Path of the pulverized coal particles to obstacles element positioned under 45° and with central angle of 8° , the paths of the colored particle diameter

Ovo je očiglednije kada se upoređuje sa česticama peska, zbog njihove mnogo veće inercije, a prikazano je na slici 4 elementa prepreka pod uglom od 55° sa centralnim uglom od 8° , za sve prečnike, gde je putanja pokazuje intenzitet brzina čestica. Jasno se može uočiti da se putanje čestica peska od $300\ \mu\text{m}$ i $1500\ \mu\text{m}$ u delu mlina u kojoj postoje elementi prepreka, veoma razlikuju. Elementi prepreka sa svojim prisustvom dalje drobe čestice ugljene prašine kao i čestice mineralne materije, ali uz pad pritiska na izlazu iz kanala za prašinu.

Uticaj veličine čestica peska na putanju u ventilacionom mlinu i kanalu za prašinu, kada se istovremeno ubrizgavaju čestice iz sva tri prečnika, prikazan je na slici 4. Slika 5 koja prikazuje putanje čestica u elementima prepreka potvrđuje da kako veličina čestica raste, povećava se i broj njihovih udara na elemente prepreka, dok manje čestice gotovo ne udaraju u barijere elementa prepreka, već se kreću praktično duž obima mlina.

This is more evident when is comparing to particles of sand, because of their much higher inertia, and is shown in Figure 4 of obstacles element at the angle of 55° with the central angle of 8° , for all there diameter, where the path are colored particles speed intensity. It can be clearly observed that the trajectory of $300\ \mu\text{m}$ and $1500\ \mu\text{m}$ of sand particles in the part of the mill in which there are obstacles elements are very different. The obstacles elements with their presence further crumble the particles of coal dust as well as the particles of mineral matter, but with the pressure drop at the exit of the dust channel.

The influence of the sand particles size on a path in the ventilation mill and the dust channel, when simultaneously injecting particles from all three diameters is shown in Figure 4. Figure 5 showing the path of particles in the obstacles elements confirms that as the particle size increases, the number of their impacts on the obstacles elements increases, while fewer particles almost do not hit the barriers of obstacles elements but are moving practically along the mill circumference.



Slika 4. Putanja čestica peska sa elementom prepreke postavljenim pod 55° i centralnim uglom od 8° , obojena putanja je za intenzitetom brzine čestica prečnika $300\ \mu\text{m}$

Figure 4. Path of sand particles with obstacles element positioned under 55° and central angle of 8° , path are colored with speed intensity for particles diameter; $300\ \mu\text{m}$

2. Modalne analize obloženih uzoraka

Eksperimentalna modalna analiza je izvedena da bi se odabrale optimalne tehnologije prevlačenja radi povećanja radnog veka elemenata u ventilacionom mlinu. Brzina i pritisak iz numeričke simulacije identifikuju delove mlina koji su najviše izloženi habanju. Proces odabira optimalnih postupaka oblaganja, dodatnih materijala i tehnologije nanošenja koji će se koristiti u eksploatacionom stanju u kasnijoj fazi eksperimenta, uradiće se na osnovu rezultata numeričkih simulacija, strukturnih i mehaničkih svojstava uzoraka iz eksperimentalnog modela obloge koji je objašnjen u ovom poglavlju.

Prodor abrazivnih čestica i visoka tvrdoća obrnuto su proporcionalni tvrdoći površinskih slojeva [3, 22, 30-32]. Parametri koji utiču na otpornost na habanje, pored tvrdoće, su struktura, oblik, veličina i distribucija mikro-sastojaka u nanetom sloju [3, 12-27]. Otpornost na habanje nantet legure zavisi od mnogih drugih faktora kao što su tip, oblik i raspodela tvrdih faza, kao i žilavost i otpornost matrice na naprezanje [4]. U dosadašnjim istraživanjima analizirana je široka skala dodatnih materijala otpornih na habanje [12] i za potrebe ovog eksperimenta, jedna grupa dodatnih materijala za testiranje modela je odabrana i analizirana potencijalna implementacija u funkcionalnom testiranju.

Urađeno je modalno ispitivanje makrostrukture, napravljeni su dijagrami raspodele tvrdoće, zona površinskog sloja i zone toplotne uticaja (HAZ). Mikrostrukturne analize su dobijene sken elektronskom mikroskopijom (SEM) i EDS

2. Modal analyses of coated samples

Experimental modal analysis is preformed to select optimal coating technologies to increase working life of elements in ventilation mill. Speed and pressure from numerical simulation has identify parts of mill which are the most exposed to wear. The process of selection the optimal coating procedures, filler materials and coating technology which will be used in exploitation condition in later stage of experiment, it will be done based on the results of numerical simulation, structural and mechanical properties of samples from experimental coating model which is explained in this chapter. The penetration of the abrasive particles and high hardness is inversely proportional to the hardness of the surface layers [3, 22, 30-32]. Parameters which effect on the wear resistance beside hardness are the structure, shape, size and distribution of micro constituents in the coated layer [3, 12- 27]. The wear resistance of a coated alloy depends on many other factors such as the type, shape and distribution of hard phases, as well as the toughness and strain hardening behavior of the matrix [4]. In previous research wide scale of filler materials resistance to wear is analyzed [12] and for the purpose of this experiment, one group of filler material for model testing is selected and analyzed potential implementation in the functional testing.

Modal testing of macrostructure has been done, diagrams of distributions of hardness have been made, zone of the surface layer and Heat affected zone (HAZ). Microstructuaral analyses were



analizom. Izbor dodatnog materijala i postupaka nanošenja koji će potencijalno koristiti i primenjivati u redizajnu radnih elemenata ventilacionog mlina se može postići iz rezultata ovog istraživanja.

Optimizacija performansi ventilacionog mlina postiže se korelacijom neizbežnog tehnološkog procesa i stanja glavnih radnih delova. Numerička simulacija višefaznog toka, zasnovana na raspoloživim parametrima, ukazuje na moduse loma komponenti sistema i olakšava uklanjanje uzroka.

2.1 Eksperimentalni postupak modalnog testiranja

Modalno ispitivanje se vrši na uzorcima obloženim adekvatnim slojem. Uzorci dimenzija 200x200x15 mm, koji su napravljeni od toplo valjanog čeličnog lima S355J2G3 (ASTM 572), pripremljeni su i korišćeni kao supstrati. Da bi se sprečilo formiranje uključaka u nanetom materijalu, pre procesa nanošenja, uklonjeni su oksidni slojevi sa površine supstrata brušenima. Pre nanošenja, uzorci su prethodno zagrejani na $T_p = 160-170^\circ\text{C}$. Korišćen je konvencionalni postupak nanošenja (zavarivanja): ručno elektrolučno zavarivanje (MMA) i zavarivanje punjeno žicom (FCAW), plazma nanošenje i HVOF (gasni plamen velike brzine High Velocity Oxi-Fuel) proces. Nakon procesa nanošenja, uzorci su hlađeni na vazduhu do sobne temperature.

Dodatni materijali, korišćeni u ovom radu, predstavljeni su u Tabeli 1, sa postupcima za nanošenje, oznakama i nominalnim hemijskim sastavima kao i komercijalnim nazivom proizvođača Castolin Eutectic Co, Ltd, Beč. Najvažniji uslov procesa nanošenja je nizak stepen mešanja i proizvodni troškovi potrošnog materijala..

obtained with scanning electron microscopy (SEM) and with EDS analysis. The choice of filler materials and coating procedures which will potentially use and applied in the redesign of ventilation mill working elements it can be done from the results of this research.

Optimization of ventilation mill performances is achieved by correlating the inevitable technological process and the state of the main working parts. Numerical simulation of multiphase flow, based on the available parameters, indicated the modes of failure system components and facilitates the removing of causes.

2.1 Experimental procedure of modal testing

Modal testing is carried on the samples coated with adequate layer. Samples dimensions 200x200x15 mm, that are made of hot-rolled steel sheet S355J2G3 (ASTM 572), were prepared and used as substrates. In order to prevent the inclusion formation in the material deposits, prior to process of coating, the oxide layers were removed from the substrate surface by means of the grinding. Before coating, samples are preheated at $T_p = 160-170^\circ\text{C}$. Conventional process of coating (welding) was used: manual metal arc welding (MMA) and flux core wire welding (FCAW), plasma coating, and HVOF (High Velocity Oxy-Fuel) process. After process of deposition samples with coatings were air-cooled down to the room temperature.

The filler materials, used in this paper, were presented in Table 1, with coating procedures, signs and nominal chemical compositions and commercial name manufactured by Castolin Eutectic Co, Ltd, Vienna. The most important condition of processes of deposition is that have low degree of mixing and the manufacturing cost of deposition consumables.

Coating Material Materijal za nanošenje	Nominal chemical compositions Nominalni hemijski sastav (M*/C and M/Fe wt.% ratio)	Process hardfacing Postupak tvrdog navarivanja
PG6503	Ni-Cr-Bo-Si/ 60% WC	Plasma process
55586C	CoCrFeCW/ WC	HVOF
4010 EC	Fe-Cr-C-Si/Ti 0.18 (7.0 and 0.6)	MMA
4395N	Fe-C-Cr-Ni-Mo-W-B	FCAW

Tabela 1. Materijali i postupci za nanošenje
Table 1. Materials and coating g procedures



2.1.1 Mikrostrukturalna analiza i ispitivanje tvrdoće

Uzorci za analizu strukture i tvrdoće izrađeni su rezanjem vodenim mlazom u ravni upravnoj na površinu nanosa. Dobijeni poprečni preseki se bruse brusnim papirima SiC do P-1200 i poliraju suspenzijama glinice do 1 μm . Mikrostrukturalna ispitivanja su izvedena na poliranim uzorcima nagriženim 3% nitalom. Mikrostrukture nanetih uzoraka su posmatrane skenirajućim elektronskim mikroskopom (SEM), a njihov hemijski sastav je ispitivan pomoću energetsko-disperzivne spektroskopije (EDS). SEM-EDS analiza je omogućila stvaranje elektronskih slika koje su omogućile morfološki opis različitih faza nanosa i EDS mape sastava korišćene za kvalitativno opisivanje hemijskih varijacija u mikrostrukturi. Takođe, merenja mikrotvrdoće u poprečnom preseku obloženih uzoraka napravljena su pomoću Vickersovog testa HV 10

2.1.1 Microstructural Analysis and Hardness Test

Samples for structure and hardness analyses were carried out by the water jet on the plane perpendicular to the coating surface. The obtained cross-sections are ground with SiC abrasive papers down to P-1200 and polished with alumina suspensions down to 1 μm . Microstructural tests were carried out on polished samples etched with a solution of 3% Nital. The microstructures of coated specimens were observed by scanning electron microscope (SEM) and their chemical compositions were examined by energy-dispersive spectroscopy (EDS). The SEM-EDS analysis was creating electron imaging allowed different phase's morphologic description of the coatings and EDS compositional maps were used to qualitatively describe chemical variations in the microstructure. Also, the measurements of micro-hardness in the cross section of coated samples were made using a Vickers hardness tester HV 10.

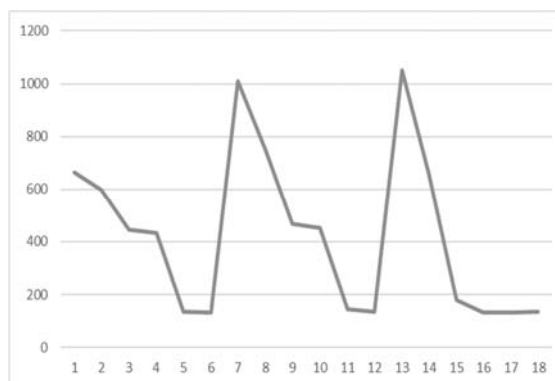
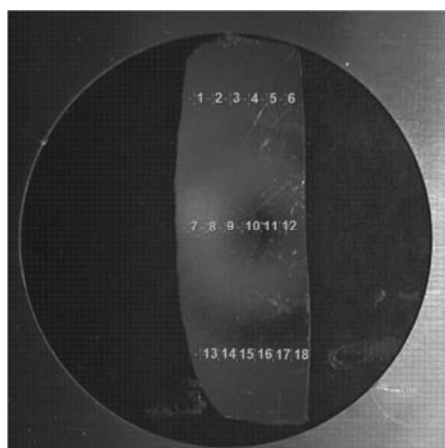
Coating material Naneti materijal	Thickness of layer in mm Debljina sloja	Degree of mixing, % Stepen mešanj	Hardness, HV10 Tvrdoća
PG6503	≈ 4.5	11	750-1049
55586C	$\approx 0.5-0.7$	10	644-701
4010 EC	≈ 5.2	20	887-1028
4395N	≈ 5	10	918-1091

Tabela 2. Materijali i postupci za nanošenje

Table 2. Materials and coating g procedures

Nizak stepen mešanja (11% i 10%) se postiže u uzorcima obloženim dodatnim materijalima PG6503, 55586C i 4395. Maksimalna tvrdoća se postiže u uzorcima obloženim legurom 4395 (MMA) i 4010EC. Merenje tvrdoće obavlja se na svim uzorcima i opseg vrednosti je prikazan u tabeli 2. Vrednosti tvrdoće zavise od tačke koja se ispituje, naneti slojevi su veoma krhki i zavise od mogućnosti uređaja. Proces merenja je izveden je po poprečnom preseku modalno obloženih uzoraka.

The low degree of mixing (11% and 10%) is achieved in coated samples with filler material PG6503, 55586C and 4395. The maximum of hardness is achieved in samples coated with alloy 4395 (MMA) and 4010EC. Measurement of hardness distribution is done for all samples and range of values is presented in the Table 2. Values of hardness depend of point which is tested, coating layers is very tick and depend if the device possibilities. Process of measurement has been done thru cross section of modal coated samples.



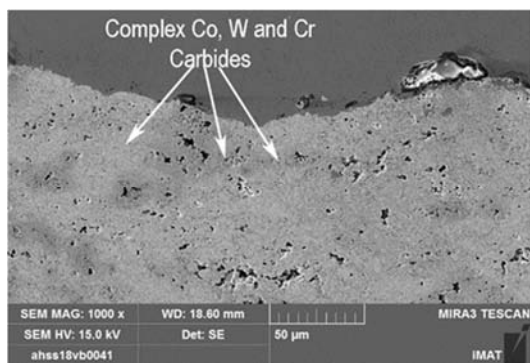
Slika 5. Makrostruktura i distribucija tvrdoće na poprečnom preseku uzorka sa dodatnim materijalom PG 6503

Figure 5. Macrostructure and hardness distribution on the sample cross section done with filler material PG 6503.

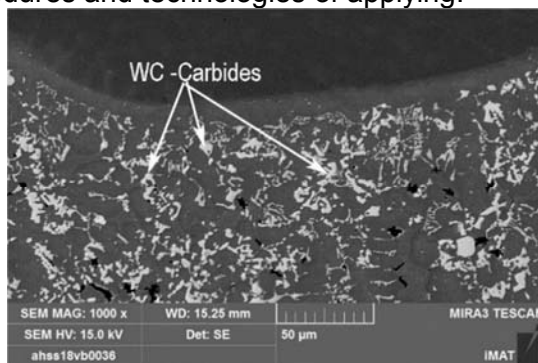


Karakteristika nanetih slojeva i varijacije tvrdoće mogu se objasniti raspodelom različitih faza duž dubine nanosa, kao što je očigledno iz mikrostrukturnog istraživanja. Makrostruktura i merenje raspodele tvrdoće preseka metaliziranog uzorka sa tvrdom prevlakom od dodatnog materijala PG 6503 postupkom metalizacije plazma lukom, prikazani su na slici 5. Vrednosti tvrdoće svih uzoraka date su u tabeli 2. Dijagram na slici 5 pokazuje da u blizini površine, tačke 7 i 13 imaju najviše vrednosti tvrdoće i više od 1000 HV. Rezultati prikazani u tabeli 2 ukazuju na to da dodatni materijali 4010 EC i 4395N pokazuju relativno homogenu raspodelu tvrdoće i mikrostrukture u poprečnom preseku i mnogo veće vrednosti tvrdoće u odnosu na druga dva uzorka. Vrednosti tvrdoće u ta dva uzorka sa dodatnim materijalima 4010 EC i 4395N su veće 20-40%. Pored toga, interval tvrdoće u poprečnom preseku je veći za 10-80%. Ta dva uzorka imaju mnogo veće vrednosti stepena mešanja osnovnog i dodatnog materijala, zbog konvencionalnih postupaka nanošenja (zavarivanja). Vrednosti tvrdoće se razlikuju iako neki dodatni materijali imaju slično hemijsko jedinjenje. To su posledice različitih postupaka oblaganja i tehnologija primene.

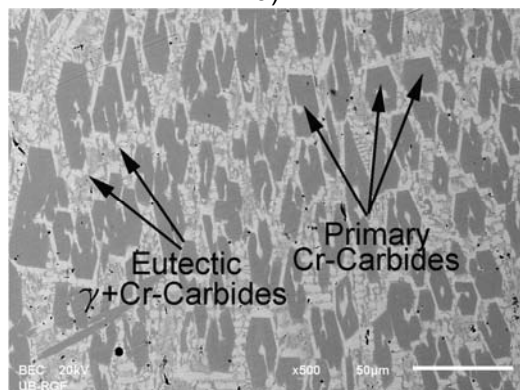
The characteristic of coated layers and the variation in hardness can be explained by the distribution of the different phases along the depth of the coated deposit, as it was evident from microstructural investigation. Macrostructure and measurement of hardness distribution of the metalized sample cross section with a hard coating with filler material PG 6503 done with plasma metallization is presented in Figure 5. Hardness values of all samples are given in the table 2. Diagram in figure 5 indicates that in near surface areas, points 7 and 13 has the highest values of hardness in the more than 1000 HV. Results show in the Table 2 indicates that a filler material 4010 EC and 4395N, show relatively homogenous distribution of hardness and microstructure in the cross-section and much higher values of hardness relative to other two samples. Values of hardness in those two samples with filler materials 4010 EC and 4395N are higher in 20 – 40%. Besides that, hardness interval in cross section is higher for 10 – 80%. Those two samples have much higher values of degree of mixing base material and filler material because are done by conventional process of coating (welding). Values of hardness are different in fact that some filler materials have similar chemical compound. This is consequences of different coating procedures and technologies of applying.



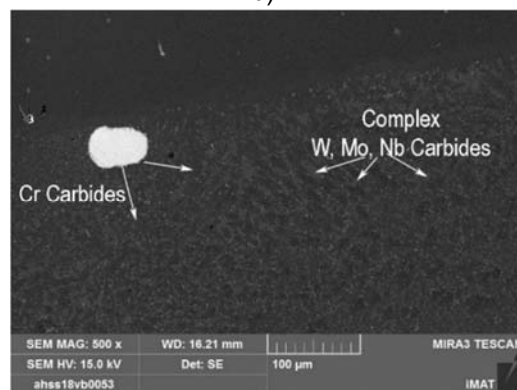
a)



b)



c)



d)

Slika 6. Strukture uzoraka a) – PG6503, b) 55586C, c) 4010 i d) 4395 tvrdi navar
Figure 6. The structures of the samples, a) – PG6503, b) 55586C, c) 4010 and d) 4395 hardfaced coatings

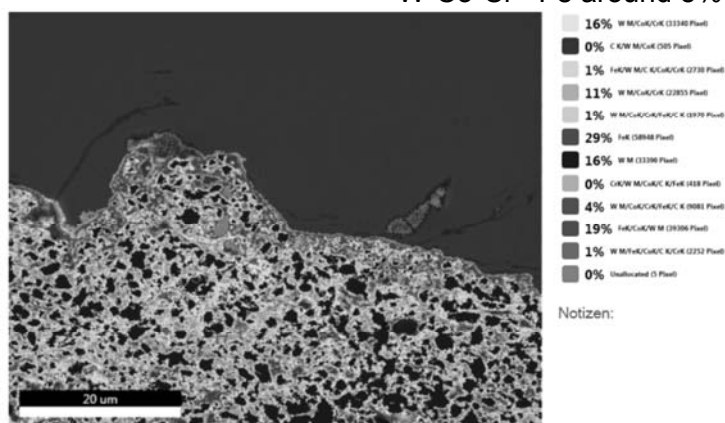


SEM mikrografije sa EDS različitih faza obloženih uzoraka dodatnim materijalom PG6503, prikazane su na slici 6. EDS podaci, prikazani u tabeli 3, ukazuju na različite sastave osnove i prisustvo karbida u nanetom sloju. Struktura blizu površine uzorka sa PG 6503 sastojala se od velikih zrna WC- tačka 2 (svetla faza, slika 7a) i EDS spektra (slika 7b i 7c) ugrađenih u matricu na bazi Ni (tamna faza, slika 7a) i EDS spektar (Slika 7d) u kojima je Fe rastvoren u velikoj količini, dok su Si i B rastvoreni u manjim količinama. Na mnogim lokacijama su uočene i male čestice WC, crvolikog oblika i slučajne orijentacije.

Raspodela velikih čestica WC ($120 \pm 31 \mu\text{m}$) bila je nejednaka u pravcu debljine prevlake, ali je njihovo prisustvo bilo najveće u površinskom području PG 6503 sloja. Pri očvršćavanju javljaju se kompleksni karbidi skoro eutektičke strukture i dominantno prisustvo oštih primarnih Cr-karbida, Cr-borida (slika 6a). U uzorku obloženom sa PG 6503 primetno je prisustvo sitnih ojačavajućih čestica borida / karbida na bazi hroma i njihovo malo rastojanje čestica koje efektivnije ojačava matricu na bazi Ni.

Slika 5b prikazuje strukturu materijala 55586C. Nanošenje materijala pokazuje homogene strukture uz prisustvo poroznosti. Matrica ovog sloja je na Fe bazi a sa eutektičkim W karbidima. Analizirajući sliku 6. može se videti prisustvo kompleksnih Co i Cr karbida. Uzorak pokazuje homogenu raspodelu karbida sa poligonalnim i sfernim oblikom. Tokom procesa nanošenja, stvoreni su vrlo složeni karbidi, dominantno izgrađeni sa W, ali sa spektrom različitih složenih struktura. Plave faze na slici 6 pokazuju dominantno eutektički W-karbid u prisustvu od oko 16%. Ostali kompleksni karbidi su W-Co-Cr oko 27%, Fe-Co-W oko 19%, W-Co-Cr - oko 5% prisustva.

SEM micrographs with EDS of different phases of coated samples with filler material PG6503 are shown in Figure 6. The EDS data, shown in table 3, indicate on different matrix compositions and presence of carbides in coated layer. The near-surface structure of PG 6503 coating consisted of large WC grains point 2 (light phase, Figure 7a) and EDS spectrum (Figure 7b and 7c) embedded in the Ni-based matrix (dark phase, Fig. 7a) and EDS spectrum (Figure 7d) in which Fe was dissolved in a major amount, whereas Si and B were dissolved in minor amounts. In many locations, the small, worm-like, and random-oriented WC particles were also observed. The distribution of large WC particles ($120 \pm 31 \mu\text{m}$) was non-uniform in coating's thickness direction but their presence was largest in the near-surface region of PG 6503 coating. During solidification achieves also complex carbides the near-eutectic structure and dominant presence of blade-like primary Cr-carbides, Cr-borides (Figure 6a). In sample coated with PG 6503 is observed the presence of small chromium-based boride/carbide reinforcing particles and their short distance between particle which strengthened more effectively the Ni-based matrix. The Figure 5b shows the structure of the material 55586C. Deposition of material shows homogenous structures with presence of porosity. Matrix of this coating is Fe base matrix with eutectic W carbides. Analyzing the figure 6. it can be seen presence of complex Co and Cr carbides. Coated sample show a homogeneous distribution of carbides with polygonal and spherical shape. During the process of deposition it's created very complex carbides, dominantly built with W but it crates various spectrums of complex structures. Blue phases on Figure 6 shows dominantly eutectic W-carbide and presence is around 16%. Other complex carbides are W-Co-Cr around 27%, Fe-Co-W around 19%, W-Co-Cr -Fe around 5% of presence.



Slika 7. Uzorci obloženi dodatnim materijalom 55586C mapiranje struktura
Figure 7. Samples coated with filler material 55586C mapping of structures.

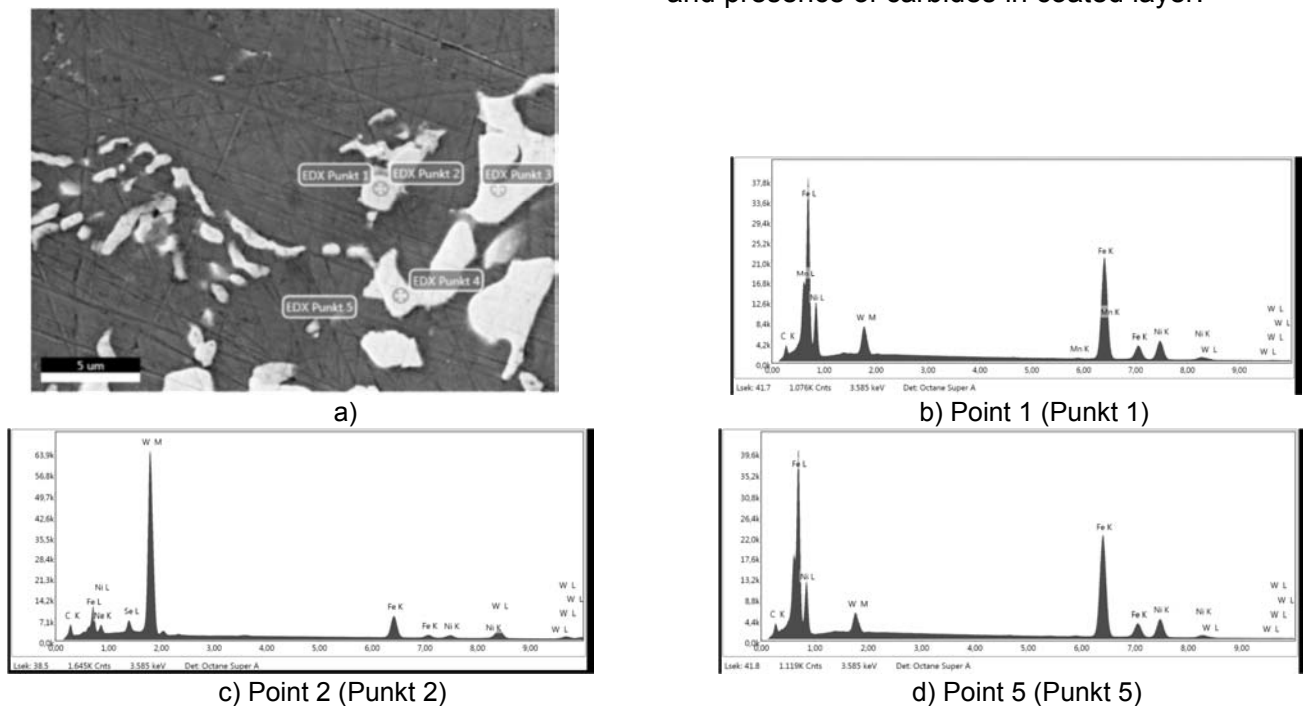


Struktura dobijenih 4010 obloga sadrži veće šipkaste primarne Cr-karbide sa potpunim odsustvom morfologije tipa lopatice (Slika 5c). Ovi rezultati su u saglasnosti sa dosadašnjim nalazima istraživanja [12, 17, 35] u kojima dodavanje ugljenika olakšava prelazak iz oštrice prema morfologiji nalik štapu. Morfologija nalik štapu je superiorna kada se razmatraju primene u trošenju. Povećanje zapreminske frakcije Cr-karbida je verovatno rezultat dodavanja ugljenika i hroma [17, 18, 26, 35]. Istaknuto je da se veliki primarni karbidi, koji su identificirani kao (Cr, Fe) $7 C_3$, formiraju iz rastopa elektrode (za tvrdo navarivanje) i pokazuju stubičasti rast sa šestougaoim poprečnim presekom.

Međutim, uzorci obloženi dodatnim materijalima 4395, pokazuju homogenu raspodelu karbida sa poligonalnim i sferičnim oblikom. Prikazani podaci EDS ukazuju da je naneti sloj, faza sa visokim sadržajem W, Cr, Nb, Mo i C. Prisutni karbidi su primarni, specijalni karbidi tipa WC, MoC, NbC, kompleksni karbidi Fe₃(V, Mo) $3C$ i Cr-karbidi [3, 12, 26], Kako se povećava frakcija specijalnog i kompleksnog karbida, poboljšava se tvrdoća i otpornost na habanje [1-3]. SEM mikrografije sa EDS različitih faza, uzoraka obloženih sa PG6503, prikazane su na slici 8. EDS podaci, prikazani u tabeli 3, ukazuju na različite sastave matrice i prisustvo karbida u nanetom sloju.

The structure of the obtained 4010 coatings comprises a larger rod-like primary Cr-carbides with the total absence of the blade-like type of morphology (Figure 5c). These results are in agreement with previous research findings [12, 17, 35] in which the addition of carbon facilitates transition from blade-like towards the rod-like morphology. The rod-like morphology is superior when wear applications are considered. The increase of the Cr-carbides volume fraction is probably the result of the carbon and chromium addition [17, 18, 26, 35]. It has been pointed out that large primary carbides, which are identified to be (Cr, Fe) $7 C_3$, are formed from the melt of the coating (hardfaced) electrodes and exhibit columnar growth with a hexagonal cross section.

However, the samples coated with filler materials 4395 show a homogeneous distribution of carbides with polygonal and spherical shape. The EDS data shown indicate that coated layer is phase with high content of W, Cr, Nb, Mo and C. Present carbides are the primary, special carbides type WC, MoC, NbC, complex carbides Fe₃(W, Mo) $3C$ i Cr-carbides [3, 12, 26], As the special and complex carbide fraction increases, hardness and wear resistance improve [1-3]. SEM micrographs with EDS of different phases of coated samples PG6503 are shown in Figure 8. The EDS data, shown in table 3, indicate on different matrix compositions and presence of carbides in coated layer.



Slika 7. a) SEM mikrografija i EDS struktura uzorka obloženog sa PG6503
Figure 7. a) SEM micrograph and EDS structure of the coated sample PG6503



3. Zaključak

Numeričke simulacije višefaznog toka izvedene su za ventilacioni mlin u elektrani Kostolac B. Rezultati dobijeni numeričkom simulacijom jasno pokazuju da CFD metode izvršene u ANSYS FLUENT-u pružaju detaljne analize protoka u ventilacionom mlinu sa elementima prepreka u kućici. Numerička analiza određuje uglove pod kojima čestice smeše napuštaju kućicu ventilacionog mlina.

U ovom radu je analiziran odgovarajući ugao ugradnje elemenata prepreka u objektu ventilacionog mlina radi povećanja efikasnosti brušenja. Najviša efikasnost brušenja ventilacionog mlina će biti ako se elementi prepreka na kućici postavljaju direktno u pravcu kretanja većih delova ugljene prašine. Ugao pod kojim čestice uglja napuštaju kućicu mlina uveliko zavisi od koeficijenta trenja između ovih čestica i udarne ploče. Za koeficijent trenja od 0,6, ugao pod kojim ugljena prašina napušta kanal za prašinu iznosi 29,5o, dok za koeficijent trenja 0,8 taj ugao ima vrednost 25,7o.

Definisano je nekoliko geometrija prepreka elemenata pravougaonog preseka, promenjen je njihov ugao i stepen podešavanja. Za centralni ugao od 8o i 12o položaj elemenata prepreka bio je na 45o, 55o.

Zapreminski udeo ugljene prašine na ulazu u ventilacioni mlin ima vrednost $3,44 \times 10^{-5}$, dok pesak $3,48 \times 10^{-5}$. Kada je prisutan fiksni ugao elemenata prepreka, primećuje se da povećanje koraka između elemenata dovodi do mnogo ravnomernije raspodele ugljene prašine u području radnog točka, između elemenata prepreka i kanala za prašinu. Uticaj ugla postavljanja elemenata prepreka i njihovih koraka analizira se modelom mešavine, koja daje pouzdane vrednosti statičkog pritiska na izlazu iz kanala za prašinu.

Lagrangeov model za praćenje čvrstih granuliranih faza je pokazao, da se pri povećanju veličine čestica ugljene prašine, povećava broj njihovih udara na elemente prepreka, dok manje čestice, usled manje inercije, prate tok gasne faze. i kreću se duž zida ventilacionog mlina i imaju manje uglove napada na zidove kanala za prašinu. Ovo je još izraženije kod čestica peska zbog njihove veće inercije, tako da se putevi različitih prečnika čestica veoma razlikuju po površini elemenata prepreka.

Otpornost na habanje određena je veličinom, oblikom, raspodelom i hemijskim sastavom karbida, kao i mikrostrukturu matrice. Da bi se procenilo ponašanje trošenja različitih legura na bazi Fe, Ni, Co, važno je uzeti u obzir makro tvrdoću i mikrostrukturu i postaviti ih u odnos.

3. Conclusion

The numerical simulations of the multiphase flow are performed for a ventilation mill in the Kostolac B power plant. The results obtained by the numerical simulation clearly show that the CFD methods done in ANSYS FLUENT provide detailed analyses of flow in ventilation mill with obstacles element in house. Numerical analysis determines angles under which particles of mixture leave the house of ventilation mill. In this paper is done analyze appropriate angle of obstacles element installation in the house of ventilation mill to increase the grinding efficiency. The most efficiency of ventilation mill grinding will be if the obstacles elements on the house are set directly in the direction of movement of larger parts of coal dust. The angle at which coal particles leave the house of mill depends largely on the friction coefficient between these particles and the impact plate. For the friction coefficient of 0.6, the angle at which the coal dust leaves the dust channel is 29.5o, while for the coefficient of friction 0.8 this angle has a value of 25.7o. Several geometries of obstacles elements of rectangular cross-section are defined, and their setting angle and step are changed. For the central angle of 8o and 12o the position of obstacles elements was at 45o, 55o. The volume fraction of coal dust at the entrance to the ventilation mill has a value of $3.44 \cdot 10^{-5}$, and sand $3.48 \cdot 10^{-5}$. When is present the fixed angle of obstacles elements, it is noted that increasing the step between the elements leads to a much evenner distribution of coal dust in the area of the working wheel, between the obstacles elements, and in the dust channel. The influence of the angle of setting the obstacles elements and their steps is analyzed by the model of the mixture, which gives the reliable values of the static pressure at the exit of the dust channel. The Lagrange model for the tracking of solid granular phases has shown that when increasing the particle size of coal dust, the number of their impacts on the obstacles elements increases, while the smaller particles, due to less inertia, follow the flow of the gaseous phase and move along the wall of ventilation mill, and have smaller attack angles to the walls of the dust channel. This is even more pronounced in sand particles due to their higher inertia, so that the paths of different diameters particles are very different in area of obstacles elements. Wear resistance is determined by the size, shape, distribution and chemical composition of the carbides, as well as by the matrix microstructure. To evaluate the wear behavior of the different Fe, Ni, Co-based coating alloys it is Koji kriterijumi su primenjeni u selekciji: radni



uslovi, otpornost na abraziju, zahtevani kvalitet završne obrade, dozvoljena debljina, poroznost sloja i koheziona čvrstoća osnovnog i primenjenog sloja, karakteristike osnovnog materijala, oblik i veličina radnog komada i troškovi celog procesa.

U mikrostrukturi, karbidi u nanetom sloju su različitog oblika, veličine i sastava u zavisnosti od hemijskog sastava dodatnog materijala. U belim gvoždima sa visokim sadržajem Cr karbida u dominantnoj formi šipki, a u legurama legiranim sa Ti, W, Nb, B, Mo, itd. postoje i kompleksi poligonalnih karbida i sfernih veličina. Tvrdoća nanetih slojeva povećava se sa većim prisustvom složenih karbida poligonalnih i sferičnih veličina. Slojevi manje tvrdoće pokazali su manju otpornost na abrazivno trošenje, ali je zavisnost (tvrdoća od brzine istrošenosti) bila nelinearna.

Analizirajući, može se zaključiti da broj prepreka u kući ventilacionog mlina što bliže radnom točku, povećava broj mogućih sudara čestica uglja. Na ovaj način postiže se povećanje idealne površine i efikasnosti brušenja iza radnog točka sa udarnim pločama. Promenom oblika prepreka, poprečnog preseka i ugla ugradnje postiže se dodatno povećanje njegove idealne površine što poboljšava kvalitet sušenja mlina. Svi ovi rezultati učestvuju u povećanju kvaliteta ugljene prašine.

Proces protoka uglja u ventilacionom mlinu sa elementima prepreka se izbjgava nepotrebna recirkulacija čestica minerala, peska i uglja, kao i dela transportnog fluida iz separatora ugljene prašine u mlin. Na ovaj način, značajno je smanjeno trošenje radnih elemenata mlina, posebno udarnih ploča radnog točka, jer je u ovom procesu došlo do trošenja prepreka, što je produžilo preostali radni vek ovih mlinova. .

Analizom obloženih uzoraka i procesa nanošenja sloja može se zaključiti da dodatni PG6503 pokazuje najbolji potencijal otpornosti na habanje distribucijom mikrokonstituenata, gde se analizira tvrdoća i distribucija mikrokonstituenata. Ali i drugi materijali imaju dobar potencijal otpornosti na habanje. Obloženi uzorci će biti analizirani simulacijom trošenja u eksperimentalnim uslovima. Primena ovog sloja će se koristiti i za oblaganje prepreka u ventilacionom mlinu.

Primena ovih dodatnih materijala za buduće rekonstrukcije mora biti podržana dodatnim testiranjem. Ovde je moguće koristiti simulaciju trošenja u mašinama za peskarenje sa peskom kao abrazivnim medijem. Potrebno je koristiti uglove napada koji se mešaju oko elemenata prepreka dobijenih numeričkom simulacijom. Multidisciplinarna istraživanja koja se koriste u ovom radu mogu dati dobre rezultate u smislu

important to regard the macro hardness and the microstructure and to set them into relation.

The which criteria were applied in the selection: working conditions, abrasion resistance, required finishing quality, permissible thickness, porosity of the layer and cohesion strength of the base and applied layer, characteristics of the basic material, shape and size of the work piece and costs of whole process.

In the microstructure, coated carbides were noticed with different shape, size and composition depending on the chemical composition of filler material. In white irons with high contents of Cr carbides in dominate form of bars, and in alloys alloyed with Ti, W, Nb, B, Mo, etc. there are also complex of polygonal carbides and spherical sizes. Coated layers hardness increases with a greater presence of complex carbides of polygonal and spherical sizes. Coatings with lower hardness showed lower abrasive wear resistance, but the dependence (hardness vs. wear rate) was nonlinear.

Analyzing, it can be concluded that as the number of obstacles in the house of ventilation mill set as close as possible to the working wheel increases the number of possible collisions of coal particles. In this way, an increase in the ideal surface and grinding efficiency is achieved behind the working wheel with impact plates. By changing the shape of the obstacles, the cross-section and the angle of installation, an additional increase in its ideal surface is achieved, which improves the drying quality of the mill. All this results participate in an increase in the quality of coal dust.

The flow process of grinding coal in a ventilation mill with obstacles elements is avoided by the unnecessary recirculation of particles of minerals, sand and coil as well as of the part of the transport fluid from the coal dust separator into the mill. In this way, the wear of the working elements of the mill, in particular the impact plates of working wheel, has been significantly reduced, since part of this process has been brought wear of obstacles, which has prolonged the remaining working life of these mills.

Analyzing the coated samples, and process of deposition of coating it can be concluded that filler material PG6503 show best wear resistance potential by distribution of microconstituents, where is analyzed hardness and distribution of microconstituent's. But other materials also have good potential of wear resistance. Coated samples will be analyzed by simulation of wear in experimental condition. Application of this coating will be used also for coating of obstacles elements



smanjenja trošenja radnih elemenata ventilacionog mlina i produženja njihovog veka trajanja, čime se olakšava eksploatacija uglja uz manji broj zaustavljanja u eksploataciji.

Priznanja

Ovaj rad je rezultat istraživanja u okviru projekta TR 34028, kojeg finansijski podržavaju Ministarstvo prosvete, nauke i tehnološkog razvoja Srbije, Messer Tehnogas i PD TE - KO Kostolac.

4. References

1. KOZIĆ M, RISTIĆ S, PUHARIĆ M, KATAVIĆ B, PRVULOVIĆ M, "Comparison of Numerical and Experimental Results for Multiphase Flow in Duct System of Thermal Power Plant," Scientific Technical Review, Vol. 60, 2010, p. 39-47,.
2. MIRKO KOZIC, SLAVICA RISTIC, BORIS KATAVIC, MIRJANA PUHARIC, "Redesign of impact plates of ventilation mill based on 3D numerical simulation of multiphase flow around a grinding wheel" Fuel Processing Technology, FUPROC-03583; 2012, No of Pages 14,
3. Metals Handbook, 9th ed., Volume 18, Friction, lubrication and wear, ASM, Metals Park, Ohio, ISBN978-1-61503-163-4, 1993, pp. 320-380.
4. M. KAZEMPOUR • H. SHOKROLLAHI • SH. SHARAFI, The Influence of the Matrix Microstructure on Abrasive Wear Resistance of Heat-Treated Fe–32Cr–4.5C wt% Hardfacing Alloy, Tribol Lett vol.39, 2010, p. 181–192.
5. B. PERKOVIĆ, A. MAZURKIJEVIĆ, V. TARASEK, LJ. STEVIĆ, Reconstruction, and realization of the projected modernization of power block B2 in the TE Costal, Termotehnika 1, 2004, p.57–81.
6. M. KOZIĆ, S. RISTIĆ, M. PUHARIĆ, B. KATAVIĆ, M. PRVULOVIĆ, Comparison of numerical and experimental results for multiphase flow in duct system of thermal power plant, Scientific Technical Review, Vol. 60, 2010, p.39–47.
7. KAMALESH S. BHAMBARE, ZHANHUA MA, LU. PISI, CFD modeling of MPS coal mill with moisture evaporation, Fuel Processing Technology Vol. 91, 2010, pp 566–571.

in ventilation mill. The application of these filler materials for future reconstructions is must be supported with additional testing. Here is possible to use simulation of wear in sandblasting machinery with sand as abrasive medium. It necessary to use attack angles which mixture flow around obstacles elements which are obtained from numerical simulation. Multidisciplinary research used in this paper can give good results in terms of reducing the wear of the working elements of the ventilation mill and extending their lifetime, and thus facilitating coil exploitation with a smaller number of stops in exploitation.

Acknowledgements

This paper is the result of research within the project TR 34028, which is financially supported by Ministry of Education, Science and Technological Development of Serbia, Messer Tehnogas and PD TE – KO Kostolac.

8. European Product Catalogue, Wear and Fusion Technology, Castolin Eutectic International Co, Vienna.
9. YI ZHOU, ZHIQIANG HUANG, FUXIAO ZHANG, SHUANG JING, ZHEN CHEN, YACHAO MA, GANG LI, HAITAO REN, Experimental study of WC–Co cemented carbide air impact rotary drill teeth based on failure analysis, Engineering Failure Analysis, vol. 36, 2013, p. 186-198
10. Thermo investigation and analysis of boiler plant blocks B1 and B2 in Kostolac TE, PD Ltd. Production–technical sector, 2014, (internal study).
11. B. KATAVIĆ, B. JEGDIĆ, M. PROKOLAB, M. PRVULOVIĆ, STEVAN BUDIMIR, Z. MILUTINOVIĆ, Optimal Parameters Estimation by the Analytical Methods for the Welding of the GS-36Mn5 Steel, Congress Welding 2012 & NDT 2012 / Proceedings of abstracts, ISBN 987-86-82585-10-7, 2012. p 51-51
12. CHAO LIU, DONGXIANG JIANG , FULEI CHU, JINGMING CHEN, Crack cause analysis of pulverizing wheel in fan mill of 600 MW steam turbine unit, Engineering Failure Analysis, vol. 42, No. 2, 2014, p. 60-73
12. A. ALIL, B. KATAVIĆ, M. RISTIĆ, D. JOVANOVIĆ, M. PROKOLAB, S. BUDIMIR, M. KOČIĆ, Structural and mechanical properties of different hard welded coatings for impact plate for ventilation mill, Welding and Material Testing 3 ,2011, p.7–11 (ISSN 1453-0392),.
13. E. GERCEKCIOGLU, D. ODABAS, E. DAGASAN, Effect of Impact Angle on the Erosive Wear Rate of Dual- phase (DP) AISI 1020, AISI 1040, AISI 4140 and AISI 8620 Steels, Journal of the Balkan Tribological Association, 2009, p. 25-35, Book 1, (ISSN 1310-4772)
14. M.F. BUCHELY, J.C. GUTIERREZ, L.M. LE´ON, A. TORO., "The effect of microstructure on abrasive wear of hardfacing alloys", Wear 259, 2005, p.52-61.



L. Weingrill^{1,a}, M. Schwald^{1,b}, D. Frühstück¹, C. Faustmann¹, N. Enzinger^{1,c}

GMA root welding of pearlitic rails using magnetic arc deflection

GMA zavarivanje korena perlitnih šina korišćenjem skretanja magnetnog luka

Originalni naučni rad / Original scientific paper

Rad je u izvornom obliku objavljen u okviru 71. IIW godišnje Skupštine i međunarodne konferencije održane na Baliju-Indonezija 15-20. Jula 2018

Rad primljen / Paper received:

April 2019.

Adresa autora / Author's address:

¹ IMAT Institute of Material Science, Joining and Forming, Graz University of Technology, Austria
^aleonhard.weingrill@tugraz.at,
^bmartin.schwald@tugraz.at,
^cnorbert.enzinger@tugraz.at

Ključne reči: zavarivanje šina, perlitni čelik, elektrolučno zavarivanje u zaštiti gasa, skretanje magnetnog luka

Key words: rail welding, pearlitic steel, gas metal arc welding, magnetic weld arc deflection

Abstract

In this work optimization research for automated GMA root welds of pearlitic rails of grade R260 is presented. The important novelty of the used approach consisted of weld arc deflection via an externally applied magnetic field to increase the lateral penetration at the root of a narrow gap weld. During welding tests in laboratory an optimization of parameters was carried out, which comprised: the welding current, voltage and speed, filler wire diameter, and the strength of the external magnetic field. Results were evaluated through geometrical aspects of the weld, such as the maximum achievable lateral and diagonal root penetration, the microstructure and the hardness were evaluated. Additionally, the behaviour of the process under the influence of the external magnetic field was studied using a high-speed camera. The beneficial influence of the external magnetic field could be illustrated. It was found that best results can be obtained in high welding current spray arc mode (380-400A) with the 1,6mm wire at high welding speed (65cm/min). A high and constant magnetic flux density close to the weld arc of at least 30mT and increased welding voltage (30-31V) for a longer weld arc was found to be beneficial. Applying this approach, it was possible to weld the root layer of the used pearlitic rail foot samples with a continuously penetrated root. A smooth transition at the lower edges could be achieved. The resulting microstructure inside the heat affected zone was fully pearlitic and in comparison to the currently predominant aluminothermic (AT) rail welding, as a result of lower heat input, of finer morphology. Thus hardness drops at the transition from HAZ to BM could be avoided. Furthermore, the size of the HAZ was reduced by more than 75% in comparison to an AT rail weld.

Rezime

U ovom radu prikazano je optimizaciono istraživanje za automatske GMA (elektrolučno u zaštiti gasa) zavarivanja korena perlitnih šina klase R260. Važna novina korišćenog pristupa sastoji se u skretanju luka zavarivačkog preko spoljašnjeg magnetnog polja radi povećanja bočnog uvarivanja u korenu uskog žljeba. Tokom testova zavarivanja u laboratoriji izvršena je optimizacija parametara, koja je obuhvatila: struju zavarivanja, napon i brzinu, prečnik žice kao dodatnog materijala i jačinu spoljašnjeg magnetnog polja. Rezultati su procenjavani kroz geometrijske aspekte šava, kao što su maksimalno ostvarivo bočno i dijagonalno uvarivanje korena, mikrostruktura i tvrdoća. Pored toga, proučavane su pojave tokom procesa pod uticajem spoljašnjeg magnetnog polja pomoću kamere velike brzine. Može se ilustrovati povoljan uticaj spoljašnjeg magnetnog polja. Utvrđeno je da se najbolji rezultati mogu postići u režimu strujnog luka (380-400A) sa visokom strujom zavarivanja sa 1,6mm žicom pri velikoj brzini zavarivanja (65c/min). Utvrđeno je da je korisna visoka i konstantna gustina magnetnog fluksa u blizini luka zavarivanja od najmanje 30mT i povećanog napona zavarivanja (30-31V) za duži luk zavarivanja. Primenom ovog pristupa moguće je zavariti koreni prolaz korišćenih perlitnih šina sa kontinuirano uvarenim krenom. Može se postići glatki prelaz na donjim ivicama. Dobijena mikrostruktura unutar zone pod uticajem toplote bila je potpuno perlitna i u poređenju sa trenutno prevladavajućim aluminotermijskim (AT) zavarivanjem šina, kao rezultat manjeg unosa toplote, finije morfologije. Tako se može izbeći pad tvrdoće na prelazu iz ZUT u OM. Šta više, veličina ZUT je smanjena za više od 75% u odnosu na AT šav na šinama.



1. Introduction

Continuously welded rail strings have become common worldwide in order to meet increased demands in safety, travelling comfort as well as to increase the lifetime of the rails and undercarriage through reduced dynamic loading and thus reduced wear and rolling contact fatigue. Welds still represent weak spots of the rail lines due to softening of the base material inside the HAZ. Furthermore, even complete failures of the rail at welds is encountered statistically reproducible more often due to weld defects [1]–[4]. In general, the weldability of the most commonly used pearlitic rails is very limited. One of the main reasons for that is these rail steels' very high carbon-content (0,8% and above). The second one is that welding in the track in remote location offers little to no infrastructure and can bear harsh environment conditions. Aluminothermic (AT) welding is for almost 120 years the preferred process for joining rails in the track accounting for about 3 Mio welds per year worldwide [5]. Due to its very small demand in equipment and thus very good practicability in remote places of little to no infrastructure and also harsh environmental conditions it still represents the state of the art for rail welding on track. Therein especially the relatively big tolerance allowance for the width of the weld gap play an important role. Furthermore, there are practically no investment costs involved, especially when compared to flash butt welding. Some disadvantages remain: A manual process depends on the welder's skills and thus always brings an uncertainty factor in quality. Reduced toughness of the weld is more likely because of the casting microstructure. Furthermore, there is an unavoidable hardness drop at the outer limits of the heat affected zone (HAZ)[6]–[8], as a result of the process' high heat input.

Gas metal arc (GMA) welding is presumably a very good alternative process to overcome the mentioned disadvantages of AT-welding. First of all, the welding parameters (including the filler material) can be adapted layer by layer. Thus the mechanical properties of the joint can be adjusted to the locally most suitable needs, such as high strength and ductility for improved fatigue strength at the root of the joint, high hardness and wear resistance at the head of the rail. If used properly many possible influencing parameters of GMAW can be used to optimize the process. Furthermore, GMA welding can be very well automatized, thus the welding results are more reliable. Still, some welding technological challenges have to be overcome in order to implement a new process for

1. Uvod

Kontinuirano zavarene trake za šine postale su uobičajene u svetu kako bi se zadovoljili povećani zahtevi u pogledu sigurnosti, udobnosti putovanja i povećanja životnog veka šina i donjeg postroja kroz smanjeno dinamičko opterećenje a time smanjeno trošenje i zamor kontaktnog kotrljanja. Zavareni spojevi i dalje predstavljaju slabe tačke pruga zbog omekšavanja osnovnog materijala unutar ZUT-a. Šta više, čak i potpuni lomovi šine na zavarenim spojevima se češće susreću a statistički se pojavljuju zbog defekata u šavu [1] - [4]. U principu, zavarljivost najčešće korišćenih perlitnih šina je veoma ograničena. Jedan od glavnih razloga za to, je veoma visok sadržaj ugljenika u železničkim čelicima (0,8% i više). Drugi je da zavarivanje na stazi u udaljenim lokacijama nudi malo ili nimalo infrastrukture i može podneti teške uslove okoline. Aluminotermijsko (AT) zavarivanje je skoro 120 godina poželjan proces spajanja šina na stazi sa oko 3 miliona zavarenih spojeva godišnje širom sveta [5]. Zbog svoje veoma male potražnje u opremi i samim tim veoma dobre praktičnosti u udaljenim mestima sa malo ili nimalo infrastrukture i oštrim uslovima okruženja i dalje predstavlja stanje tehnike za zavarivanje na železnici. Posebno važnu ulogu ima relativno velika tolerancija širine zazora. Štaviše, praktično nema troškova ulaganja, posebno u poređenju sa elektrootpornim zavarivanjem varničnjem. Neki nedostaci ostaju: Ručni proces zavisi od veština zavarivača i stoga uvek donosi faktor neizvesnosti u kvalitetu. Smanjena žilavost šava je verovatnija zbog mikrostrukture livenja. Osim toga, postoji neizbežan pad tvrdoće na spoljašnjim granicama zone pod uticajem toplote (HAZ) [6] - [8], kao rezultat visokog unosa toplote u procesu. Zavarivanje električnim lukom u zaštiti gasa (GMA) je verovatno veoma dobar alternativni proces za prevazilaženje pomenutih nedostataka AT-zavarivanja. Prvo, parametri zavarivanja (uključujući dodatni materijal) mogu se prilagoditi sloj po sloj. Tako se mehanička svojstva spoja mogu prilagoditi lokalno najpogodnijim potrebama, kao što su visoka čvrstoća i duktilnost za poboljšanu čvrstoću na zamor u korenu spoja, visoka tvrdoća i otpornost na habanje na glavi šine. Ako se pravilno koriste mnogi mogući parametri koji utiču na GMAW mogu se koristiti za optimizaciju procesa. Osim toga, GMA zavarivanje se može veoma dobro automatizovati, tako da su rezultati zavarivanja pouzdaniji. Ipak, neki tehnološki izazovi za zavarivanje moraju biti prevaziđeni kako bi se implementirao novi proces zavarivanja na železnici.



rail welding. One of them is to achieve a proper geometry of the weld. This aspect is most important but due to very restricted accessibility also most difficult to achieve at the root layers. In order to obtain lateral penetration arc manipulation is necessary. Out of this background the aim of this work is defined: The root geometry for a GMA weld of pearlitic rail should be improved by applying a – to this domain - new approach. The objective is to experimentally realize a proof of concept through laboratory test welds. The focus is set to the root welding only.

2. Approach to solution

The chosen approach consists on the one side of a two pass per layer weld sequence with a detailed parameter optimization for each of the passes individually. On the other side it consists of the manipulation of the electromagnetic forces of the weld arc and also the electric current carrying droplets in transfer and melt pool by an external magnetic field. As a result, the arc and weld are laterally deflected and thus the lateral penetration improved for each section of the weld. Compared to alternative deflection methods of the weld arc by mechanically bending the tip of the filler wire this approach bears two major advantages: First, the magnetic unit is principally very simple and robust. This keeps investment costs down, no additional mechanical parts are necessary which can wear and could become faulty during intensive use. Second, through controlling the current in the magnetic coils in magnitude and direction, also the external magnetic field can be altered during the welding process and thus the weld arc can be adjusted in-situ to one's needs.

3. Experimental procedures

The used setup for the welding experiments is schematically depicted in Fig. 1. A Fronius TPS 4000 CMT® welding device and water cooled GMAW narrow gap welding torch were used. The torch was mounted in neutral position on a stationary stand together with horizontal, but slightly sidewise tilted magnetic yoke. The legs of the magnetic yoke were aligned parallel to the welding direction to create the intended parallel magnetic field and thus the lateral deflection of the weld arc. The tips of the legs were positioned symmetrically and closest possible to the tip of the filler wire.

Jedna od njih je da se postigne pravilna geometrija šava. Ovaj aspekt je najvažniji, ali je zbog veoma ograničene pristupačnosti i najteže postići na korenim slojevima. Da bi se dobilo bočno uvarivanje neophodna je manipulacija lukom.

Iz ove pozadine je definisan cilj ovog rada: geometrija korena za GMA zavarivanje perlitne šine treba da se poboljša primenom novog pristupa. Cilj je eksperimentalno ostvariti dokaz koncepta kroz laboratorijske testove zavarenih spojeva. Fokus je podešen samo na zavarivanje korena.

2. Pristup rešenju

Odabrani pristup sastoji se na jednoj strani od dva prolaza po jednom sloju zavarivanja sa detaljnom optimizacijom parametara za svaki od pojedinačnih prolaza. S druge strane, on se sastoji od manipulacije elektromagnetskih sila zavarivačkog luka, kao i od kapljica koje u spoljašnjem magnetnom polju nose kapljice pri prenosu i rastopljenju kupki. Kao rezultat, luk i šav su bočno pomereni i na taj način je bočno uvarivanje poboljšano za svaki deo šava. U poređenju sa alternativnim metodama skretanja luka zavarivanja mehaničkim savijanjem vrha žice, ovaj pristup ima dve glavne prednosti: prvo, magnetna jedinica je uglavnom jednostavna i robusna. Time se smanjuju investicioni troškovi, ne zahtevaju se dodatni mehanički delovi koji se mogu nositi i mogu postati neispravni tokom intenzivne upotrebe. Drugo, kontrolisanjem struje u magnetnim kalemima po magnitudi i smeru, kao i spoljašnje magnetno polje koje se može menjati tokom zavarivanja i tako se luk može podesiti na licu mesta, prema potrebama.

3. Eksperimentalni postupci

Korišćena postavka za eksperimente zavarivanja shematski je prikazana na slici 1. Korišćeni su Fronius TPS 4000 CMT® uređaj za zavarivanje i vodeno hlađeni GMAW gorionik za zavarivanje. Gorionik je montiran u neutralnom položaju na stacionarnom postolju zajedno sa horizontalnim, ali blago bočnim nagibom magnetnog jarma. Noge magnetnog jarma su poredane paralelno sa pravcem zavarivanja da bi se stvorilo predviđeno paralelno magnetno polje, a time i bočno otklanjanje luka zavarivanja. Vrhovi nogu su postavljeni simetrično i najbliže moguće vrhu žice za zavarivanje.

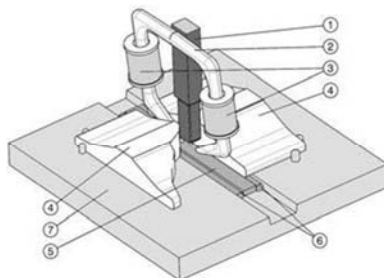


Fig. 1. Schematic of experimental setup. 1... welding torch 2... magnetic yoke 3... coils 4... rail foot samples 5... steel strip for weld pool backing 6... ceramic tube for backing laterally penetrating weld metal 7... support plate.
Slika 1. Shema eksperimentalne postavke. 1... gorionik za zavarivanje 2... magnetni jaram 3... zavojnice 4... uzorci stopala šine 5... čelična traka za podlošku kupki 6... keramička cev za podlošku bočno uvarivanje metala šava 7... noseća ploča.

The magnetic field was introduced with the help of two coils of 500 windings, which were clamped to the upper part of each of the two legs of the yoke. Electric current to the windings was supplied by a separate laboratory power unit (not depicted in Fig. 1) with adjustable DC-voltage and current. The weld sample were made of R260 60E1 rails. The nominal chemical composition of this steel is given in Table 1.

Magnetno polje je uvedeno uz pomoć dve zavojnice od 500 namotaja, koji su bili pričvršćeni za gornji deo svake od dve noge jarma. Električna struja do namotaja je snabdevena odvojenim laboratorijskim izvorom snage (koja nije prikazana na slici 1) sa podesivim DC-naponom i strujom. Uzorak zavarenog spoja je izrađen od R260 60E1 šina. Nominalni hemijski sastav ovog čelika dat je u tabeli 1.

Main alloying elements weight -%					
C	Si	Mn	P max.	S max.	Cr
0,62-0,80	0,15 - 0,58	0,70-1,20	0,025	0,025	≤0,15

Table 1. Nominal chemical composition of used rail steel according to [9]
Tabela 1. Nominalni hemijski sastav korišćenog čelika za šine prema [9]

The weld flanks were vertical straight in as sawed condition with no specific preparation. To guarantee reproducible positioning, the weld samples were clamped on a dedicated support plate with alignment pins on each side. Clamping was done with standard knee levers. In order to fit the weld pool backing a clearance was milled into the support plate. A 16mm wide steel strip of S355 structural steel was placed at the bottom side of the 16mm wide weld gap to support the weld pool. Its top surface was evenly levelled to the bottom surface of the rail foot samples, so that the edges of strip and samples touched in one line one each side. The strips thickness was varied throughout the experiments from initially 1,5mm to finally 6mm. The strip was fixed to the samples with two manual TIG tack welds on the bottom surface on each side. Furthermore, on both sides of the weld gap at the bottom edges ceramic tubes were pressed into the remaining gap between steel strip, samples and support plate, in order to back the penetrating weld metal there.

Šavovi za zavarivanje su bili vertikalnog pravca u uslovima testerisanja bez specifične pripreme. Da bi se garantovala reproduktivna pozicioniranost, uzorci zavarenih spojeva su bili pričvršćeni na namenskoj nosećoj ploči, čivijama za poravnavanje na svakoj strani. Stezanje je izvršeno standardnim polugama. Da bi se podloška zavarivačke kupke uklopila u zaštitnu ploču, zazor je izbrušen u nosećoj ploči. Čelična traka širine 16 mm od konstrukcionog čelika S355 postavljena je na donju stranu zazora širine 16 mm kako bi se osigurala zavarivačka kupka. Njena gornja površina je ravnomerno poravnata sa donjom površinom uzoraka stopala, tako da su ivice trake i uzorci dotakli jednu liniju sa svake strane. Debljina traka je varirala tokom eksperimenata od inicijalno 1,5 mm do 6 mm. Traka je pričvršćena na uzorke sa dva pripoja ručnim TIG zavarivanjem na donjoj površini, sa svake strane.

Osim toga, na obe strane zazora na donjim ivicama, keramičke cevi su utisnute u preostali zazor između čelične trake, uzoraka i noseće ploče, kako bi se tamo uvario metal šava.

-Kraj 1. dela NASTAVAK U SLEDEĆEM BROJU



¹ Vladimir Khomenko

New highly productive technology of combined welding of main pipelines of major diameter

Nove visoko produktivne tehnologije kombinovanog zavarivanja glavnih cevovoda velikog prečnika

Stručni rad / Professional paper

Rad je u izvornom obliku objavljen u Zborniku sa 4. IIW Kongresa zavarivanja Jugoistočne Evrope „Safe Welded Construction by High Quality Welding“ održanog u Beogradu 10-13. Oktobra 2018

Rad primljen / Paper received:

April 2019.

Ključne reči: magistralni gasovodi; zavarivanje; visokoproduktivne tehnologije

Adresa autora / Author's address:

¹ Russian Union Of Oil And Gas Constructors

Key words: main gaspipelines; welding; highproductive technologies

In the course of construction of the pipelines, welding of circular nonrotative pipe joints is one of the main working operations. This operation is carried out using different methods. The welding technology of each method has special features which make it attractive for using at one or another facility depending on specific conditions of the construction work. Meanwhile, improvement of the well-known and development of new, more universal technologies of welding, is an important task of the pipeline construction. The urgent character of this work grows increasing in view of proposed construction of major pipelines with a high work pressure and the wall thickness of 30 mm and more for pipes of big diameter. At the same time the requirements to reliability are increasing greatly. In these circumstances the effectiveness of welding may be approved only by using highly productive automatic methods of welding which ensure welded joints of high quality. The purpose of this work is development of highly productive technology of automatic welding of nonrotative joints at the main pipelines of big diameter with increased thickness of pipe walls for gas and oil transportation. The technology ensures welded joints of high quality.

The analysis of different aspects of the well-known automatic methods of pipe welding has allowed to determine the direction in which the task can be resolved. To do it the combined method of welding including press and arc welding turned out to be the most optimum one. As a result we recommend a new method of automatic pipe welding. It consists of two welding methods widely tested in practice: flash-butt welding (FBW) and self-shielded flux-cored arc welding by forced formation of weld (SFCAW). By combining these

U toku izgradnje cevovoda, zavarivanje kružnih nerotirajućih spojeva cevi je jedna od glavnih radnih operacija. Ova operacija se izvodi različitim metodama. Tehnologija zavarivanja svake metode ima posebne karakteristike koje je čine privlačnom za korišćenje na jednom ili drugom objektu u zavisnosti od specifičnih uslova građevinskih radova. U međuvremenu, unapređenje poznatih i razvoj novih, univerzalnijih tehnologija zavarivanja, važan je zadatak izgradnje cevovoda. Hitni karakter ovih radova, raste s obzirom na predloženu izgradnju glavnih cevovoda sa visokim radnim pritiskom i debljinom zida od 30 mm i više za cevi velikog prečnika. Istovremeno, zahtevi za pouzdanošću se uveliko povećavaju. U takvim okolnostima, efikasnost zavarivanja može se odobriti samo uz upotrebu visoko produktivnih automatskih metoda zavarivanja koje osiguravaju visok kvalitet zavarenih spojeva.

Svrha ovog rada je razvoj visokoproduktivne tehnologije automatskog zavarivanja nerotirajućih spojeva na glavnim cevovodima velikog prečnika sa povećanom debljinom zidova cevi za transport gasa i nafte. Tehnologija osigurava visok kvalitet zavarenih spojeva.

Analizom različitih aspekata poznatih automatskih metoda zavarivanja cevi, omogućeno je odrediti smer u kojem se zadatak može rešiti. Za to je optimalna bila kombinovana metoda zavarivanja, uključujući pritisak i elektrolučno zavarivanje. Kao rezultat toga preporučujemo novi način automatskog zavarivanja. Sastoji se od dve široko testirane metode zavarivanja: sučeono zavarivanje varničanjem (FBW) i zavarivanja samosaštitnom punjenom žicom uz pomoć prisilnog oblikovanja šava (SFCAW). Kombinovanjem ovih metoda zavarivanja postignut je pozitivan efekat



methods of welding a positive effect has been achieved which was difficult to achieve by using each of these methods apart. It has allowed, as it will be shown later, to refine the welded joints and to increase the efficiency of welding. The Figure 1 shows a macrosection of a pipe weld executed by using the proposed method.

During SFCAW the main difficulty is to obtain sustained performance of joints taking into account difficulties when welding the root pass. In order to refine the root pass complicated technical devices are to be used such as in-tube centralizer with backing ring, in-tube welding machines with programmably-changeable parameters of welding depending on position of weld, as well as other means not always ensuring positive result. As a result while using different SFCAW technologies for the root pass welding the rejection rate increases which results in additional expenses on joints repairing and not only makes work efficiency lower, but brings down the reliability of the pipelines. That is why one needed new technical ideas to resolve the problem of the root pass welding. Using of FBW to weld the root pass is expedient because of physic peculiarity of this method. While using this method the conditions of obtaining a high-quality connection at any section of the joint are identical and do not depend on its position. This method does not require any devices for weld formation. The welding machine itself acts as centralizer of the pipe edges being welded. In the process of welding of each joint the computer-based monitoring of the welding process parameters takes place. The quality of the weld is evaluated on the basis of results of the monitoring. This method of evaluation is about 100% trustworthy, which is confirmed by exhaustive studies and long-term practice of welding of pipes of different diameters and of other pieces. This method is based on the direct correlation of occurrence of certain welding defects compared to level of deviation of the main process parameters from the set points determined for the optimum welding process. The industry practice confirms the high reliability of the weld joints executed by using FBW. More than 70 thousand kilometers of different pipelines were welded using this method. They have been trouble-free operated for some decades in different climatic conditions including major pipelines 1420 mm in diameter in Arctic regions of West Siberia. And at the same time not a single joint was subjected to heat treatment. The problem with FBW is, that according to certain normative documents, an additional processing step is recommended at welding pipes big diameter operated at

koji je teško ostvariti korišćenjem svake od ovih metoda, odvojeno. To je omogućilo, kao što će biti prikazano kasnije, da poboljša zavarene spojeve i poveća efikasnost zavarivanja. Slika 1 prikazuje makropreseki šava cevi zavarene predloženim postupkom.

Tokom SFCAW glavna poteškoća je da se postigne neprekidno izvođenje spojeva uzimajući u obzir teškoće pri zavarivanju korenog prolaza. U cilju poboljšanja korenog prolaza koriste se složeni tehnički uređaji kao što su centralizator sa prstenima, unutarcevne zavarivačke mašine sa programabilnim promenljivim parametrima zavarivanja u zavisnosti od položaja zavarivanja, kao i druga sredstva koja ne obezbeđuju uvek pozitivan rezultat. Kao rezultat toga, korišćenjem različitih SFCAW tehnologija za zavarivanje korenog prolaza povećava se odbacivanje, što rezultuje dodatnim troškovima popravke spojeva i ne samo da smanjuje efikasnost rada, već smanjuje i pouzdanost cevovoda. Zato su bile potrebne nove tehničke ideje da bi se rešio problem zavarivanja korena.

Upotreba FBW-a za zavarivanje korenog prolaza je korisna zbog fizičke posebnosti ove metode. Pri primeni ove metode, uslovi dobijanja kvalitetne veze na bilo kom delu spoja su identični i ne zavise od njegovog položaja. Ova metoda ne zahteva nikakve uređaje za stvaranje šava. Sama aparatura za zavarivanje funkcioniše kao centralizator ivica cevi. U procesu zavarivanja svakog spoja odvija se kompjutersko praćenje parametara zavarivanja. Na osnovu rezultata monitoringa se procenjuje kvalitet zavara. Ovaj metod vrednovanja je 100% pouzdan, što potvrđuju iscrpne studije i dugogodišnja praksa zavarivanja cevi različitih prečnika i drugih delova. Ova metoda se zasniva na direktnoj korelaciji pojavljivanja određenih grešaka u zavarivanju u odnosu na nivo odstupanja glavnih procesnih parametara od podešenih tačaka za optimalni proces zavarivanja. Industrijska praksa potvrđuje visoku pouzdanost zavarenih spojeva izvedenih pomoću FBW. Ovom metodom je zavareno više od 70 hiljada kilometara različitih cevovoda. Oni su bez problema radili nekoliko decenija u različitim klimatskim uslovima, uključujući glavne cevovode prečnika 1420 mm u arktičkim regionima zapadnog Sibira. U isto vreme nijedan spoj nije podvrgnut termičkoj obradi.

Problem sa FBW-om je u tome što se prema određenim normativnim dokumentima preporučuje dodatni korak obrade kod cevi velikog prečnika koje rade na temperaturi od 20°C ispod nule. Ovaj korak predstavlja lokalnu termičku obradu zavarenog



of temperature 20° C below zero. This step represents a local heat treatment of welded joint in order to improve the characteristics of the impact resistance. Thereupon these characteristics are considered to correspondent to the level of impact resistance required for joints welded by arc welding (regardless of the welding method the impact resistance of welds is lower than that of the main metal). The studies are evidence of the fact that filling of the SFCAW welding groove after welding of the FBW root pass make it possible to refuse the above mentioned recommendation and to increase the impact resistance of metal of the FBW joint thanks to effect of the SFCAW thermal cycle. And, taking into account that to weld the root pass using FBW method it is necessary to prepare the pipe edges before welding, that is to reduce the profile to be welded (Fig. 1), it becomes possible to use FBW for welding of pipelines with wall thickness of 30 mm and more (at present the construction bodies possess powerful welding machines K 700, but they are destined for welding of pipes 1420 mm in diameter with wall thickness up to 20 mm).

Look-alike operation on special machine work of butt ends of pipes (pipe bearing faces) before welding is obligatory operation at gas metal arc welding. For example, it is provided in one of the most widely used technologies abroad – “CRC-Evans AW”. Pendant beveling machines are applied as standard equipment for these purposes. The estimation of performance of the suggested method of welding of circumferential welds was given on the sector segments cut from pipes of hardness group X60 ... X70, diameter 1420 mm, 1220 mm with wall thickness 16 ... 26 mm. Extent of sector segments on a circumference compounded 200 ... 300 mm. By earlier executed studies it is established that such extent of a separate member of pipes is minimally admissible. At such extent of sector segments, conditions of formation of joints at resistance welding remain practically the same, as at welding of bulk cross-section pipes. Quality of weld joints was evaluated according to requirements of normative documents of OAO Gazprom and the Russian standards, and also by studies of fractured surfaces of the samples especially shattered on a zone of joint.

Ultrasonic and X-ray inspections were used as non-destructive methods of estimation of welding quality. The most effective quality monitoring of the suggested method of pipe welding is x-ray. The basic requirement for its application is qualitative removal of internal rags which is formed during welding from flash metal, heated to high temperature,

spoja radi poboljšanja karakteristika otpornosti na udar. Smatra se da su ove karakteristike u skladu sa nivoom otpornosti na udar koji je potreban za zavarene spojeve elektrolučnim zavarivanjem (bez obzira na metodu zavarivanja, otpornost na udar šava je manja od otpornosti osnovnog materijala). Istraživanja pokazuju da ispuna žljeba SFCAW-om, nakon zavarivanja korenog prolaza FBW-om, omogućava odbijanje gore navedene preporuke i povećanje otpornosti zavarenog spoja FBW-om, zahvaljujući efektu termičkog ciklusa kod SFCAW. Uzimajući u obzir da je za zavarivanje korenog prolaza pomoću FBW-om potrebno pripremiti ivice cevi pre zavarivanja, odnosno smanjiti profil koji se zavaruje (slika 1), moguće je koristiti FBW za zavarivanje cevovoda. sa debljinom zida od 30 mm i više (trenutno građevinska tela poseduju moćne aparate za zavarivanje K 700, ali su namenjena za zavarivanje cevi prečnika 1420 mm debljine zida do 20 mm).

Višekratni rad na specijalnim radnim mašinama sučeonih krajeva cevi (površine ležišta cevi) pre zavarivanja je obavezan pri elektrolučnom zavarivanju u zaštiti gasa. Na primer, obezbeđena je u jednoj od najčešće korišćenih tehnologija u inostranstvu - “CRC-Evans AV”. Kao standardna oprema za ove namene primjenjuju se mašinski privesci za nagib.

Procena performansi predloženog načina zavarivanja kružnih šavova dat je na segmentima koji su izrezani iz cevi grupe tvrdoće X60... X70, prečnika 1420 mm, 1220 mm sa debljinom zida 16... 26 mm. Obim segmenata na obodu je povećan za 200... 300 mm. Ranijim studijama utvrđeno je da je takav opseg odvojenog dela cevi minimalno dopušten. U takvom obimu segmenata, uslovi formiranja spojeva pri elektrootpornom zavarivanju ostaju praktično isti, kao i kod zavarivanja celih prečnika cevi.

Kvalitet zavarenih spojeva procenjen je prema zahtevima normativnih dokumenata OAO Gazprom i ruskim standardima, kao i studijama o lomovima površina uzoraka posebno oštećenih u zoni spoja. Kao metode bez razaranja za ocenu kvaliteta zavarivanja korišćene su ultrazvučna i rendgenska ispitivanja. Najefikasniji monitoring kvaliteta predloženog načina zavarivanja cevi je rendgen. Osnovni uslov za njegovu primenu je kvalitativno uklanjanje unutrašnjih “krpica” koje se formiraju pri zavarivanju od metala, zagrejanog do visoke temperature, i dotoka rastopljene kupke (sl. 2). Količina krpica proporcionalno smanjuje debljine



and inflows of the molten puddles (Fig. 2). The quantity of rags relieves proportionally to decrease of thickness of welded sections. At poor removal of rags, in x-ray pictures in the center of a joint there can be a crack-tip opening displacement from upset surfaces of joined metals. This method allows also supervising quality of removal of an internal rag.

The form and parameters of edge preparation on the suggested method are specified by requirements of FBW and EAW. At the initial stage the problem was put forward of defining the most rational sizes of lugs (Fig.3), which execute a role of a root bead: thickness – h and width - l . Magnitude - h was chosen on the basis of greatest possible thermal influence by SFCAW on metal structure of a zone of welding of the root bead executed by FBW. Studies have demonstrated that at thicknesses of lugs at the size of 8-14mm this condition is met to the full. At smaller thicknesses of a root bead the danger of burn increases at intensive mode of EAW. The magnitude - l was determined based on flashing allowances and welding upset at FBW and the set spacing interval between edges for qualitative implementation of SFCAW.

The basic requirement to FBW in this case is supply of qualitative joints at the minimal shrinkage allowance on welding. It is caused by minimization of machine work of edges before welding and obtaining of joints with small rags. The last is the relevant factor not only for development of technology for removal of rags, but also for a choice of mode of SFCAW. A choice of optimum welding conditions was executed on sector segments of the above-stated sizes, the butt ends of which were treated up to thickness of 6 – 14 mm. Such sizes of a root bead for the pointed thickness are the most rational, proceeding from technological reasons. Welding of samples was effected on various modes, differing both in shrinkage allowances on welding, and other key parameters. Study of quality of weld joints has allowed determining FBW modes of root beads of various thicknesses, providing obtaining of qualitative joints at the minimal shrinkage allowances. Results of experimental works have demonstrated that at applicable proportions of key parameters of a mode, the minimal shrinkage allowance on welding will be so much the less than the lug is thinner. Hence, in this case, machine work of butt ends of pipes on depth (width of a lug on generant of pipe) will be the least. On the other hand, the more thickness of a lug under a root bead, the less is treating of butt ends on wall thickness of a pipe, but the shrinkage allowance is

preseka zavarenih profila. Pri lošem uklanjanju krpica, na rendgenskim slikama u središtu spoja može doći do otvaranja vrha prsline od površina spojenog metala. Ova metoda omogućava i nadzor kvaliteta uklanjanja unutrašnjih krpica.

Oblik i parametri pripreme ivica po predloženoj metodi su određeni zahtevima FBW i EAW. U početnoj fazi postavljen je problem definisanja najracionalnijih veličina ušica (sl.3), koje obavljaju ulogu korena: debljina - h i širina - l . Magnituda - h izabrana je na osnovu najvećeg mogućeg toplotnog uticaja SFCAW na strukturu zone zavarivanja korenog prolaza izvedenog FBW-om. Istraživanja su pokazala da se kod debljine ušica veličine 8-14 mm, ovaj uslov u potpunosti ispunjava. Pri manjim debljinama korenog zavara na intenzivnom režimu EAW-a raste opasnost od pregorevanja. Magnituda - l određena je na osnovu dozvoljenog odstupanja varničenja i podešavanja zavarivanja kod FBW i intervala podešavanja zazora između ivica za kvalitetnu primenu SFCAW.

Osnovni zahtjev FBW-a u ovom slučaju je isporuka kvalitetnih spojeva pri minimalno dozvoljenom skupljanju pri zavarivanju. To je uzrokovano minimiziranjem mašinske obrade ivica pre zavarivanja i dobijanja spojeva s malim krpicama. Posljednji je relevantan faktor ne samo za razvoj tehnologije za uklanjanje krpica, već i za izbor načina rada SFCAW. Na segmentima navedenih dimenzija, izvršen je izbor optimalnih uslova zavarivanja, čiji su krajevi obrađeni do debljine 6-14 mm. Takve veličine korenog prolaza za pomenutu debljinu su najracionalnije, iz tehnoloških razloga. Zavarivanje uzoraka vršeno je na različitim režimima, koji se razlikuju i kod dozvoljenih skupljanja pri zavarivanju i kod drugih ključnih parametara. Ispitivanje kvaliteta zavarenih spojeva omogućilo je određivanje FBW režima korenog prolaza različite debljine, čime se dobijaju kvalitetni spojevi pri minimalno dozvoljenom skupljanju.

Rezultati eksperimentalnih radova pokazali su da će pri odgovarajućim odnosima ključnih parametara režima, minimalno dozvoljeno skupljanje pri zavarivanju biti manje ako su ušice tanje. Dakle, u ovom slučaju, mašinska obrada krajeva cevi na dubini (širina ušice generatora cevi) će biti najmanje. S druge strane, što je veća debljina ušice ispod korenog prolaza, manje je tretiranje sučeljenih krajeva na debljini zida cevi, ali se dopušteno skupljanje uvećava, što dovodi do povećanja dubine obrade sučeljenih ivica. Tako će praktično biti identičan radni unos mašinske obrade čeonih krajeva cevi u odnosu na kombinovano zavarivanje u optimalnim odnosima debljine - h i širine - l . Izuzetak mogu biti modovi sa uvećanim



augmented thereat that leads to magnification of depth treating of butt ends. Thus, labor input of machine work of butt ends of pipes with reference to the combined welding at optimum proportions of thickness - h and widths - l will be practically identical. Exception can be modes with the augmented flashing allowance. For example, it is probable at big enough gap between butt ends of pipes on any local section before welding. Application as baseline alternative at the combined method of self-shielded flux-cored arc welding of pipes is tied up to features of FBW. As already mentioned above, FBW joints after welding have rags. At welding industrial butt joints of pipes under classic FBW technology, the rags are completely removed both from outboard, and from the interior of a butt joint. If prepared edges after welding of a root bead to be cleaned of rags (Fig. 2), then SFCAW is executed on usual technology and the mode is basically determined by the geometrical sizes of the remained part of edge preparation. However, if the rag is not removed, the weld procedure by self-shielded flux-cored arc welding is changed with particular conditions of welding. In this case, a special flux-cored wire with increased redox power in the molten bath is applied. As a result of the thermal and metallurgical processes taking place in the molten bath, the rags are melted, and oxides pass into slag, which is shaped on a surface of a joint weld. X-ray inspection has demonstrated that in this case also there are no major defects in a joint weld. In case, when the rags inside of a joint can be removed, other methods for infill of welding grooves can be used. In this case a corresponding method of edge preparation shall be applied. If rags inside the joint is removed, other methods of welding for welding groove filling can be applied. In this case relevant edge preparation for this method shall be prepared. In particular full-scale pipe diameter 1220x20 mm steel X70 were welded combination welding with flux-cored wire welding filling in protective gases. SFCAW procedure was arranged on the basis of the required effect of the thermal cycle on FBW root pass metal regarding the rags. At the same time much attention was paid to evaluation of factors influential for joint weld forming. Analysis of quality of joints welded with different allowance under FBW and different energy deposition under SFCAW showed that the most critical factor if rags exist is finite length of root pass L_{fin} (Fig. 1). This comes from the fact that under certain conditions FBW rags can turn out to be clamped between groove edges (Fig. 2). That is why SFCAW process is complicated and poor fusions can appear in joint

dopuštenim varničenjem. Na primer, verovatno je da je dovoljan veliki razmak između krajeva cevi na bilo kom lokalnom delu, pre zavarivanja.

Primena kao osnovne alternative kod kombinovane metode zavarivanja cevi samozaštitnom žicom vezana je za odlike FBW-a. Kao što je već spomenuto, FBW spojevi nakon zavarivanja imaju krpice. Pri zavarivanju sušeonih spojeva industrijskih cevi klasičnom FBW tehnologijom, krpice se u potpunosti uklanjaju iz spoljašnjeg i unutrašnjeg dela sušeonog spoja. Ako se pripremljene ivice nakon zavarivanja korenog prolaza očiste od krpica (sl. 2), tada se SFCAW izvodi uobičajenom tehnologijom i u osnovi je određen geometrijskim veličinama preostalog dela pripremljenih ivica. Međutim, ako se krpica ne ukloni, postupak zavarivanja samozaštitnom žicom se menja, sa posebnim uslovima zavarivanja. U ovom slučaju, primjenjuje se specijalna punjena žica sa povećanom snagom oksidoredukcije u rastopljenoj kupki. Kao rezultat termičkih i metalurških procesa koji se odvijaju u rastopljenoj kupki, krpice se tope, a oksidi prelaze u trosku, koja se stvara na površini spoja. Rendgenska inspekcija je pokazala da u ovom slučaju nema većih defekata u spoju.

U slučaju da se krpice unutar spoja mogu ukloniti, mogu se koristiti i druge metode za ispunu žljebova za zavarivanje. U ovom slučaju primenjuje se odgovarajuća metoda pripreme ivice.

Ako se uklone krpice unutar spoja, mogu se primeniti i drugi postupci zavarivanja za zavarivanje žljeba. U ovom slučaju pripremaju se odgovarajuće pripreme za ovu metodu. Cevi prečnika 1220 x20 mm od čelika X70 su zavarene kombinovanim zavarivanjem za ispunu žljeba punjenom žicom u zaštitnim gasovima.

SFCAW procedura je uređena na osnovu potrebnog efekta termičkog ciklusa na korenom prolazu izvedenom FBW-om u odnosu na krpice. Istovremeno, velika pažnja je posvećena proceni faktora koji utiču na formiranje zajedničkog spoja. Analiza kvaliteta zavarenih spojeva kod različitih odstupanja FBW-a i deponovanja različitim energijama kod SFCAW, pokazala je da je najkritičniji faktor ako postoje krpice konačne dužine korenog prolaza L_{fin} (sl.1). Ovo proizilazi iz činjenice da se pod određenim uslovima FBW krpice mogu isprečiti između ivica žljeba (sl. 2). Zbog toga je SFCAW proces, komplikovan jer može da se u spojevima pojavi lose stapanje. Da bi se izbegao nastanak takvih defekata, optimalna veličina zazora između ivica blizu njihove osnove, nakon zavarivanja korenog prolaza određena je eksperimentalno, tj. utvrđena je optimalna konačna



welds. To avoid appearance of such defects, optimum size between edges near their basis after welding of root pass was determined by an experimental approach i.e. optimal finite length of root pass was established. SFCAW procedure providing the required weld-pool volume and its modification program depending on hourly position of the arc was selected according to the number of rags at welding groove after FBW.

The special requirement of SFCAW is preparation of a part of welding groove before welding. It is connected both with peculiarity of joining under FBW and technical requirements to self-shielded flux-cored arc welding. This kind of preparation includes removal of large buildups of molten metal which can form on some sections during flashing-off from surfaces of root pass and edges. Concerning the existing welding equipment of flux cored wire the most important aspect is treatment of one quarter (1/4) part of the perimeter/diameter of welded pipes located at an hour zone from 3 to 6 hours.

The results of mechanical testing (Fig. 4) give evidence of positive effect of SFCAW thermal cycle on the structure of root pass made with FBW. Standard shock samples of root pass with sharp notch of composite joints showed average impact strength of 197.4 J/cm^2 /116.4...213.3/ at the temperature $+20^\circ\text{C}$. Usually joints welded by standard FBW method have impact strength of $40\text{...}50 \text{ J/cm}^2$ after welding at the same temperature. Impact strength of SFCAW weld at the same temperature is within limits of $108.6\text{...}115.9 \text{ J/cm}^2$ / $KCV_{\text{average}}=112.3 \text{ J/cm}^2$. These indices depend on chemical composition of the wire and can be increased by its alloying.

Strength properties of joints on test plates with section of $\delta \times 2\delta$, where δ – wall thickness of welded pipes and round pipes of 6 mm in diameter, cut out from sections of root pass and arc pass have strength from the level of standard required strength of welded pipes up to real strength of pipe metal. This depends on the level of thermomechanical strengthening of pipe metal during drawing.

Bending angle of samples cut out of the joint weld is 180° (Fig. 5).

Carried out by hydraulic and cyclic tests of full-scale pipe 1220×20 welded on the developed technology showed high their reliability (fig. 6)

Combined pipe welding layout is shown on drawing 7. The maximum effect of this method can be reached by welding of pipes of large diameter i.e. $1220\text{...}1420 \text{ mm}$, wall thickness $16\text{...}32 \text{ mm}$. Welding system Sever-1, and KCC-01 can be used

dužina korenog prolaza. SFCAW procedura koja obezbeđuje zahtevanu zapreminu zavarivačke kupke i program njene modifikacije u zavisnosti od satne pozicije luka, izabrana je prema broju krpica na žljebu za zavarivanje nakon FBW.

Poseban zahtev SFCAW je priprema dela žljeba za zavarivanje pre zavarivanja. Povezan je i sa specifičnošću spajanja FBW i sa tehničkim zahtevima za zavarivanje samozaštitnom žicom. Ova vrsta pripreme uključuje uklanjanje velikih nakupina rastopljenog metala koji mogu nastati na nekim delovima tokom varničenja sa površina korenog prolaza i ivica. Što se tiče postojeće opreme za zavarivanje punjenom žicom, najvažniji aspekt je obrada jedne četvrtine (1/4) dela perimetra / prečnika zavarenih cevi koje su u satnoj zoni od 3 do 6 sati.

Rezultati mehaničkog ispitivanja (sl.4) svedoče o pozitivnom efektu termičkog ciklusa SFCAW na strukturu korenog prolaza izvedenog FBW. Standardni uzorci za ispitivanje na udar iz korenog prolaza sa oštrim zarezom kompozitnih spojeva pokazali su prosečnu udarnu žilavost od $197,4 \text{ J/cm}^2$ /116.4...213.3/ na temperaturi $+20^\circ\text{C}$. Obično spojevi zavareni standardnom FBW metodom imaju udarnu žilavost od $40 \text{...}50 \text{ J/cm}^2$ nakon zavarivanja na istoj temperaturi. Udarne žilavost SFCAW šava na istoj temperaturi je u granicama od $108,6 \text{...}115,9 \text{ J/cm}^2$ / $KCV_{\text{prosek}} = 121,3 \text{ J/cm}^2$. Ovi indeksi zavise od hemijskog sastava žice i mogu se povećati njihovim legiranjem.

Svojstva čvrstoće spojeva na ispitnim pločama sa presekom $\delta \times 2\delta$, gde je δ - debljina zida zavarenih cevi i okruglih cevi prečnika 6 mm, izrezane iz sekcija korenog prolaza i dela koji se elektrolučno zavaruje, imaju čvrstoću nivoa standardno tražene čvrstoće zavarenih cevi do stvarne čvrstoće metala cevi. To zavisi od nivoa termomehaničkog ojačanja metala cevi tokom izvlačenja.

Ugao savijanja uzoraka izrezanih iz zavarenog spoja je 180° (sl. 5). Hidrauličkim i cikličnim testovima cevi 1220×20 zavarene razvijenom tehnologijom utvrđena je visoka pouzdanost (sl. 6). Izgled kombinovano zavarenih cevi prikazan je na crtežu 7. Maksimalni efekat ove metode može se postići zavarivanjem cevi velikog prečnika tj. $1220 \text{...}1420 \text{ mm}$, debljine zida $16 \text{...}32 \text{ mm}$. Sistem za zavarivanje Sever-1 i KCC-01 mogu se koristiti za FBW koreni prolaz. Sistem za zavarivanje Styk se može koristiti za završno zavarivanje spojeva, odnosno ispunu žljeba, samozaštitnom punjenom žicom. Ruske organizacije za izgradnju cevovoda imaju dugogodišnje iskustvo u radu ovim sistemima. Prema ovoj metodi, vreme zavarivanja



for FBW root pass. Welding system Styk can be used for completion of joint welding i.e. welding groove filing with self-shielded flux-cored arc welding. Russian pipeline construction organizations have great long-term experience of operating these systems. Under this method, root pass welding time is 60-120 seconds depending on thickness of pipes. Time of filling of one joint with two heads in one tent is 8-12 minutes (Fig. 8). Depending on the number of tents the rate of welding may reach 10-20 joints per hour. Currently, on the instructions of ПАО "Gazprom" has developed normative and technical documentation for the technology and work to design and build equipment for the industrial implementation of this technology.

CONCLUSION

1. Developed and tested in laboratory and production conditions combined method of welding of pipes, including consistent welding of two widely used in practice methods: automatic flash-butt welding and self-shielded flux-cored arc welding that makes full use of the main advantages of both methods.
2. Flash butt welding of root pass increases its quality. At the same time the welding procedure is simplified and welding efficiency grows up.
3. Use of self-shielded flux-cored arc welding for filling of welding grooves increases impact strength of root pass metal. At the same time external rags removal typical for flash-butt welding is not needed.
4. Mechanical characteristics of joints made by the combined method correspond to all requirements to joint welds including impact strength indices. Normal defects which can appear during welding can be detected with exact accuracy by traditional methods of nondestructive testing i.e. ultrasonic and x-ray tests.
5. The proposed method of combined welding is essential at increasing efficiency and quality of joint welds at construction of heavy-walled pipelines with wall thickness of 20...30 mm and above, especially at implementation of works at extreme climatic and weather conditions.
6. Technology of combination welding certified in PJSC Gazprom and allowed to use the technological instructions for Gazprom "VNIIGAZ "

korena je 60-120 sekundi u zavisnosti od debljine cevi. Vreme ispune jednog spoja sa dve glave u jednom šatoru je 8-12 minuta (sl. 8). Zavisno od broja šatora, brzina zavarivanja može da dosegne 10-20 spojeva na sat. Trenutno, prema instrukcijama PAO "Gazprom" je razvio normativnu i tehničku dokumentaciju za tehnologiju i rad na projektovanju i izgradnji opreme, uz industrijsku implementaciju ove tehnologije.

ZAKLJUČAK

1. Razvijen i testiran u laboratorijskim i proizvodnim uslovima, kombinovani postupak zavarivanja cevi, uključujući dosledno zavarivanje dvema široko primenjenim metodama u praksi: automatsko sučeono zavarivanje varničanjem i elektrolučno zavarivanje samozaštitnom punjenom žicom koje u potpunosti koristi glavne prednosti obe metode.
2. Sučeono zavarivanje varničanjem korenog prolazi povećava njegov kvalitet. Istovremeno se pojednostavljuje postupak zavarivanja i povećava efikasnost zavarivanja.
3. Korišćenje elektrolučnog zavarivanja samozaštitnom punjenom žicom za ispunu žljebova povećava udarnu žilavost korenog prolaza. U isto vreme nije potrebno uklanjanje spoljašnjih krpica tipičnih za sučeono zavarivanje varničanjem.
4. Mehaničke karakteristike spojeva izvedenih kombinovanom metodom odgovaraju svim zahtevima za zavarene spojeve, uključujući i pokazatelje udarne žilavosti. Normalni defekti koji se mogu javiti tokom zavarivanja mogu se otkriti tačnom preciznošću tradicionalnim metodama ispitivanja bez razaranja tj. ultrazvučnim i rendgenskim ispitivanjima.
5. Predloženi način kombinovanog zavarivanja je od suštinskog značaja za povećanje efikasnosti i kvaliteta zavarenih spojeva pri izgradnji cevovoda debljine zida od 20 ... 30 mm i više, posebno kod izvođenja radova u ekstremnim klimatskim i vremenskim uslovima.
6. Tehnologija kombinovanog zavarivanja sertifikovana je u PJSC Gazprom i dozvoljeno je da se koriste tehnološka uputstva za Gazprom "VNIIGAZ"

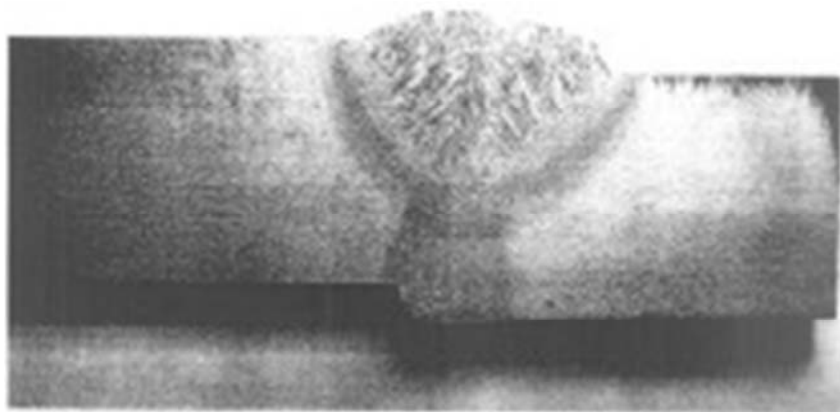


Figure. 1. Makrošlif welded joint made of combination welding.
Slika 1. Makrošlif zavarenog spoja izvedenog kombinovanim zavarivanjem

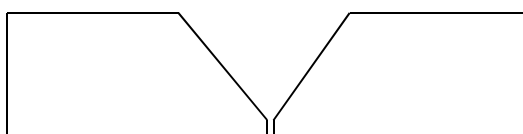
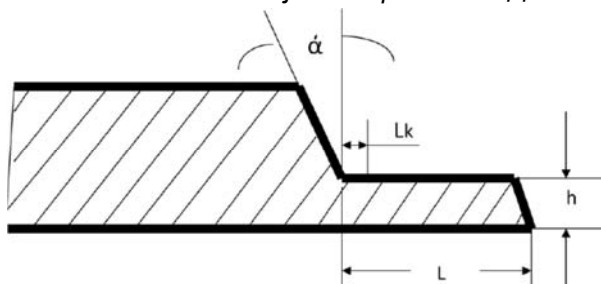


Figure. 2. Cutting edges under PЭДС.
Slika 2. Rezanje ivica prema PЭДС



\hat{h} - толщина корневого шва;
L - длина участка кромок корневого шва до сварки
L_k - длина корневого шва после сварки;
 $\hat{\alpha}$ - угол наклона кромок.

Figure. 3. The concept of cutting edges.
Slika 3. Koncept rezanja ivica

Участок сварного соединения	Показатели свойств		
	Предел текучести, МПа	Предел прочности, МПа	Ударная вязкость, Дж/см ² , 20 град, С
Основной металл	<u>564 – 582</u> 578	<u>659 – 670</u> 664	<u>108 – 116</u> 112
Участок шва выполненный Порошковой проволокой	<u>552 – 557</u> 554	<u>654 – 660</u> 655	<u>108 – 116</u> 112
Участок шва выполненный Контактной сваркой	<u>567 – 578</u> 572	<u>667 – 670</u> 668	<u>116 – 213</u> 197

Figure. 4. Mechanical properties of the weld.
Slika 4. Mehaničke osobine šava



Figure 5. Sample tested at the bend
Slika 5. Ispitana epruveta na savijanje

Результаты испытаний натуральных образцов труб

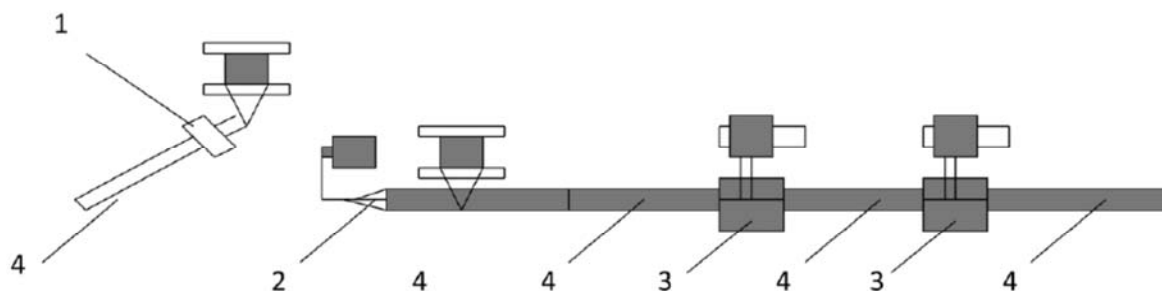
Результаты испытаний натуральных образцов труб

Номер натурального образца трубы	Испытания на прочность		Испытания на долговечность		
	Рстат, МПа	Время выдержки	Рmax/ Рmin, МПа	Мmax/ Мmin, кНм	N циклов нагружения
№ПЭК-1, №ПЭК-2 №ПЭК-3, №ПЭК-4	9,97	2 часа	8,24/0,82	1876/1129	10 000

Fig. 6 The results of hydraulic and cyclic tests of welded joints of combined welding technology



Slika 6. Rezultati hidrauličkih i cikličnih ispitivanja zavarenih spojeva izvedenih kombinovanom tehnologijom zavarivanja



- 1 – станок для обработки торцев
 2 – сварочная машина КСС
 3 – сварочная палатка для ЭДСПП
 4 – свариваемые трубы

Figure 7. Organization of work
Slika 7. Organizacija rada

Наименование операции	Время операции, мин.												
	1	2	3	4	5	6	7	8	9	10	11	12	
Установка аппарата на стык	█												
Подготовка сварочных головок к работе		█											
Сварка полукольца с одной стороны *			█	█	█	█	█	█	█	█	█	█	█
Сварка полукольца с замыканием стыка с другой стороны *				█	█	█	█	█	█	█	█	█	█
Перевод аппарата в транспортное состояние **									█	█			
Снятие аппарата и переезд к следующему стыку											█	█	

* В операциях сварки включены технологические зачистки металла и удаления шлака.

** В операцию включена смена кассет с проволокой и чистка мундштуков.

Число работающих в бригаде (всего) 7-13-17 (для 1, 2 и 3 агрегатного комплекса)

Число сварщиков операторов 2-4-6 (по 2 на агрегат)

Вспомогательный персонал 2-4-6

Инженерный персонал 1+1 (бригадир, энергетик)

Машинисты агрегатов 1-2-3

Figure 8. Ciklogramma the duration of operations when welding flux cored wire pipelines diameter 1420 mm in one working cycle

Slika 8. Ciklogram trajanja operacija pri zavarivanju punjenom žicom cevovoda prečnika 1420 mm u jednom random ciklusu



Hossein Beladi, Georgina L. Kelly and Peter D. Hodgson

Formation of ultrafine grained structure in plain carbon steels through thermomechanical processing Stvaranje ultrafinozrne strukture kod ravnih ugljeničnih čelika termomehaničkom obradom

Stručni rad / Professional paper

Rad je u izvornom obliku objavljen u časopisu *Materials Transactions*, Vol. 45, No. 7 (2004) pp. 2214 to 2218
Special Issue on Ultrafine Grained Structures #2004 The Japan Institute of Metals

Rad primljen / Paper received:

April 2019.

Adresa autora / Author's address:

School of Engineering and Technology, Deakin University,
Geelong, Australia, VIC 3217

Ključne riječi: ultrafini ferit, transformacija indukovana dinamičkom deformacijom, ravni ugljenični čelici, termomehanička obrada, sadržaj ugljenika

Key words: ultrafine ferrite, dynamic strain-induced transformation, plain carbon čeliks, thermomechanical processing, carbon content

In the present study, wedge-shaped samples were used to determine the effect of nominal equivalent strain (between 0 and 1.2) and carbon content (0.06–0.35%C) on ferrite grain refinement through dynamic strain-induced transformation (DSIT) in plain carbon čeliks using singlepass rolling. The microstructural evolution of the transformation of austenite to ferrite has been evaluated through the thickness of the strip. The results showed a number of important microstructural features as a function of strain which could be classified into three regions; no DSIT region, DSIT region and the ultrafine ferrite (UFF) grain region. Also, the extent of these regions was strongly influenced by the carbon content.

The UFF microstructure consisted of ultrafine, equiaxed ferrite grains ($<2 \mu\text{m}$) with very fine cementite particles. In the centre of the rolled strip, there was a conventional ferrite-pearlite microstructure, although ferrite grain refinement and the volume fraction of ferrite increased with an increase in the nominal equivalent strain.

1. Introduction

Ultrafine grained structures in plain carbon čeliks are gaining in popularity amongst research groups around the World as means of cutting the cost of čelik production and opening up the window of high band mechanical properties. This new generation of high strength-high toughness čeliks is recyclable and environmental friendly. There are a number of different approaches to achieve this goal, dynamic straininduced transformation (DSIT) combined with rapid cooling is a simple and practical route to produce ultrafine ferrite grains (UFF) as small as $1-2 \mu\text{m}$.¹⁻³⁾

U ovom istraživanju korišćeni su klinasti uzorci za određivanje efekta nominalne ekvivalentne deformacije (između 0 i 1.2) i sadržaja ugljenika (0.06–0.35%C) na rafinaciju feritnih zrna kroz dinamičku transformaciju (DSIT) kod ugljeničnih čelika koji se proizvode valjanjem u jednom prolazu. Razvijanje mikrostrukture transformacijom austenita u ferit je određena kroz debljinu trake. Rezultati su pokazali niz značajnih mikrostrukturnih osobina kao funkcije deformacije koje se mogu svrstati u tri oblasti; nema DSIT oblasti, DSIT oblast i oblast ultrafinozrnog ferita (UFF). Takođe, obim ovih oblasti je pod velikim uticajem sadržaja ugljenika.

Mikrostruktura UFF-a sastojala se od ultrafinih, ekvivalentnih feritnih zrna ($<2 \mu\text{m}$) sa vrlo finim česticama cementita. U centru valjane trake, postojala je konvencionalna feritno-perlitna mikrostruktura, mada je rafinacija feritnih zrna i zapreminski udeo ferita povećan sa povećanjem nominalne ekvivalentne deformacije.

1. Uvod

Ultrafinozrne strukture u ugljeničnim čelicima dobijaju na popularnosti među istraživačkim grupama širom sveta kao način smanjenja troškova proizvodnje čelika i otvaranja prostora mehaničkih svojstava visokog opsega. Ova nova generacija visoko žilavih čelika, visoke čvrstoće se može reciklirati i ekološki je prihvatljiva. Postoji više različitih pristupa za postizanje ovog cilja, dinamička transformacija (DSIT) u kombinaciji sa brzim hlađenjem je jednostavna i praktična ruta za proizvodnju ultrafinih feritnih zrna (UFF) od $1 \text{ do } 2 \mu\text{m}$.¹⁻³⁾



The DSIT exhibits a general insensitivity to variations in chemistry and could therefore be applied to the full range of čeliks.⁴⁾ This process involves a strain being applied to the metastable austenite, i.e. between the A_{e3} and A_{r3} temperature range (equilibrium and continuous cooling temperatures for austenite to ferrite transformation, respectively).⁵⁾

There is a critical condition to produce UFF through the DSIT route which could vary with thermomechanical processing history as well as čelik composition. The reduction required for UFF formation through DSIT is quite high, typically more than 40% in single pass-rolling.^{3,4)} The ultimate goal of the present work is to evaluate the effect of carbon content in conjunction with strain on the ferrite transformation characteristics through the strip thickness and detect the critical strain for DSIT and UFF formation in plain carbon steels.

2. Experimental Procedure

The composition of steels used in this study is given in Table 1. All steels are plain carbon steels with different carbon content. The hot rolling facilities, which have been used in this study, include a laboratory mill with rolls of 365mm diameter, a rolling speed of 15 rpm, a preheating resistance furnace and a fluid bed furnace with maximum working temperature of 1300 and 1100C, respectively. The wedge samples were machined to an overall size of 140mm 50mm 8mm with an angle of about 4 (Fig. 1).

DSIT pokazuje opštu neosetljivost na promene u hemijskom sastavu i stoga se može primeniti na celi opseg čelika.⁴⁾ Ovaj proces uključuje deformaciju koja se primjenjuje na metastabilni austenit, tj. između A_{e3} i A_{r3} temperaturnog raspona (ravnotežne i kontinualne temperature hlađenja) za transformaciju austenita u ferit),⁵⁾

Postoji kritično stanje za proizvodnju UFF-a preko DSIT koje može da varira zavisno od istorije termomehaničke obrade kao i sastava čelika. Sažimanje potrebno za formiranje UFF-a preko DSIT-a je prilično veliko, obično više od 40% u jednom prolazu valjanja.^{3,4)} Krajnji cilj ovog rada je da se proceni uticaj sadržaja ugljenika u sprezi sa deformacijom na karakteristike feritne transformacije preko debljine trake i detektovanja kritične deformacije za formiranje DSIT-a i UFF-a u ravnim ugljeničnim čelicima.

2. Eksperiment

Sastav čelika koji se koristi u ovoj studiji dat je u tabeli 1. Svi čelici su obični ugljeni čelici sa različitim sadržajem ugljenika. Oprema za toplo valjanje, koja je korišćena u ovoj studiji, uključuju laboratorijski valjački stan sa valjcima prečnika 365mm, brzina valjanja od 15 o/min, eletrotopnu peć za predgrevanje i peć s fluidnim slojem s maksimalnom radnom temperaturom od 1300 i 1100°C . Uzorci klinova su mašinski obrađeni do ukupne veličine 140mm x 50mm x 8mm sa uglom od oko 4 (slika 1).

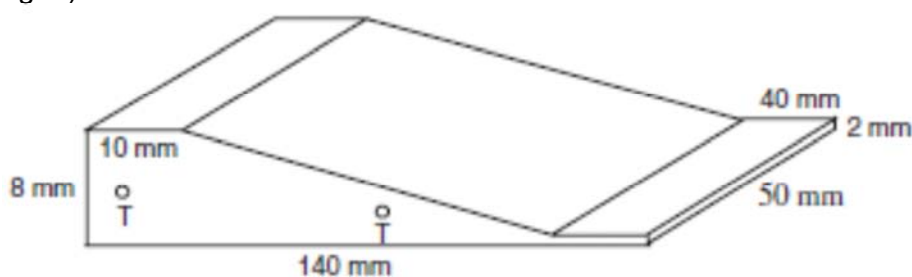


Fig. 1 Wedge specimen (T: Thermocouple position).

Slika 1. Klinasti uzorak (T: položaj termopara)

Steel	%C	%Si	%Mn	%Al	%P	%S	A_{e3} (°C)*	T_{def} (°C)	T_a (°C)	d_f (μm)
A	0.06	0.06	0.21	0.037	0.011	0.013	880	875 ± 5	1100	>120**
B	0.16	0.16	0.59	0.005	0.017	0.013	845	840 ± 5	1200	250
C	0.35	0.26	0.82	0.03	0.012	0.003	795	790 ± 5	1200	120

Table 1. The chemical composition of čeliks (in mass%).

Tabela 1. Hemijski sastav čelika (mas.%)

*The A_{e3} temperatures were calculated using the ChemSage program.

A_{e3} temperatura je izračunata korišćenjem programa ChemSage

** d could not be measured because of ultra low carbon content.

d se nije mogao izmeriti zbog ultra niskog sadržaja ugljenika



Figure 2 shows the thermomechanical processing cycles, that were applied to perform the single-pass hot rolling. The specimens were soaked at a given austenitization temperature for 15 min., resulting in austenite grain size of greater than 120 μm (Table 1). The samples were reheated in stainless steel foil bags to prevent excessive oxidation. Then, the wedge samples were rapidly placed in the fluid bed furnace at the $A_{e3}+5$ $^{\circ}\text{C}$ temperature for five minutes to stabilize the temperature for all thicknesses of the wedge sample and to avoid any temperature gradient through the thickness. Afterwards, the specimens were passed through the rolls at a given temperature (Table 1) to achieve a strip with a final thickness of 2 mm. The temperature of the specimens was measured continuously during the test by N-type thermocouples, inserted at different positions in the sides of samples (Fig. 1).

Furthermore, the surface temperature was measured by a pyrometer throughout the experiment. After deformation, the rolled strips were air cooled to room temperature.

The dimension of the wedge sample was designed based on the rolling mill capacity and to minimize the lateral spreading during rolling. However, there was still some spreading during rolling for the reductions greater than 50%.

Na slici 2 prikazani su ciklusi termomehaničke obrade, koji su primenjeni da bi se izvršilo jednokratno toplo valjanje. Uzorci su držani na datoj temperaturi austenitizacije 15 min, što je rezultovalo veličinom zrna austenita većom od 120 μm (Tabela 1). Uzorci su ponovo zagrejani u foliji od nehrđajućeg čelika kako bi se sprečila prekomerna oksidacija. Zatim, uzorci klina su brzo postavljeni u peći sa fluidizovanim slojem na temperaturi $A_{e3}+5$ $^{\circ}\text{C}$ tokom pet minuta da se stabilizuje temperatura za sve debljine uzorka klina i da se izbegne bilo kakav gradijent temperature kroz debljinu. Nakon toga, uzorci su prolazili kroz valjke na datoj temperaturi (Tabela 1) da bi se dobila traka konačne debljine od 2 mm. Temperatura uzoraka merena je kontinuirano tokom ispitivanja termoparovima N-tipa, umetnutim na različitim položajima na stranama uzoraka (slika 1).

Štaviše, površinska temperatura je merena pirometrom tokom eksperimenta. Nakon deformacije, valjane trake su hladene vazduhom do sobne temperature.

Dimenzija uzorka klina je dizajnirana na osnovu kapaciteta valjaonice i radi smanjenja bočnog rasipanja tokom valjanja. Međutim, i dalje je došlo do izvesnog širenja tokom valjanja kod sažimanja većeg od 50%.

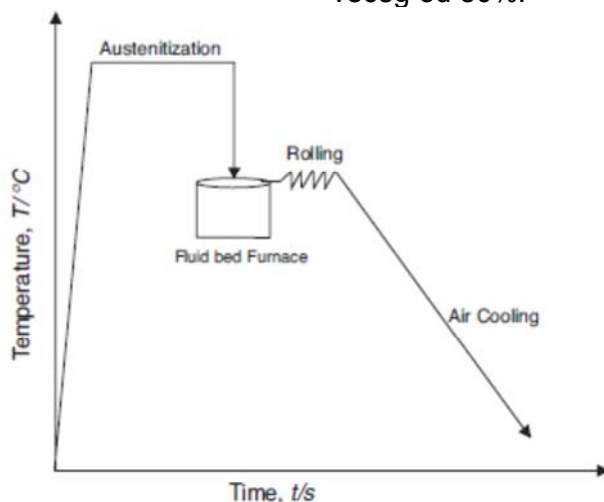


Fig. 2 Schematic representation of heat treatment and thermomechanical schedule.

Slika 2. Šematsko predstavljanje termičke obrade i termomehaničke obrade

Therefore, the width of the specimen was also measured at each location after rolling. Equation (1) as then used to estimate the equivalent strain along the rolled strip taking into account the spread.⁶⁾

$$\bar{\epsilon} = \left[\frac{4}{3} (\epsilon_t^2 + \epsilon_w^2 + \epsilon_t \epsilon_w) \right]^{1/2} \quad (1)$$

where $\epsilon_t = \ln(t_0/t_f)$ and $\epsilon_w = \ln(w_0/w_f)$ are strains in the thickness t and width w dimensions, in

Prema tome, širina uzorka je takođe merena na svakoj lokaciji nakon valjanja. Jednačina (1) se tada koristi za procenu ekvivalentne deformacije duž valjane trake uzimajući u obzir širenje.⁶⁾

$$\bar{\epsilon} = \left[\frac{4}{3} (\epsilon_t^2 + \epsilon_w^2 + \epsilon_t \epsilon_w) \right]^{1/2} \quad (1)$$

gde su $\epsilon_t = \ln(t_0/t_f)$ and $\epsilon_w = \ln(w_0/w_f)$ su deformacije u debljini t i širini w i u kojoj se indeksi



which the subscripts 0 and f refer to original and final thicknesses and widths, respectively.

Metallographic observations were made on the normal direction-rolling direction plane at a depth of between 0.1– 0.15mm below the surface of the rolled strips and at the mid thickness. The ferrite volume fraction was determined by point counting. In this study, only the volume fraction of polygonal ferrite was considered. The mean ferrite grain size was determined using the mean linear intercept method.

0 i f odnose na originalne i konačne debljine i širine. Metalografska posmatranja su obavljena po ravni normalnoj na pravac valjanja na dubini od 0,1 do 0,15 mm ispod površine valjanih traka i na srednjoj debljini. Zapreminski udeo ferita je određen brojanjem tačaka. U ovom istraživanju razmatran je samo zapreminski udeo poligonalnog ferita. Srednja veličina zrna ferita je određena korišćenjem metode srednjeg linearnog preseka.

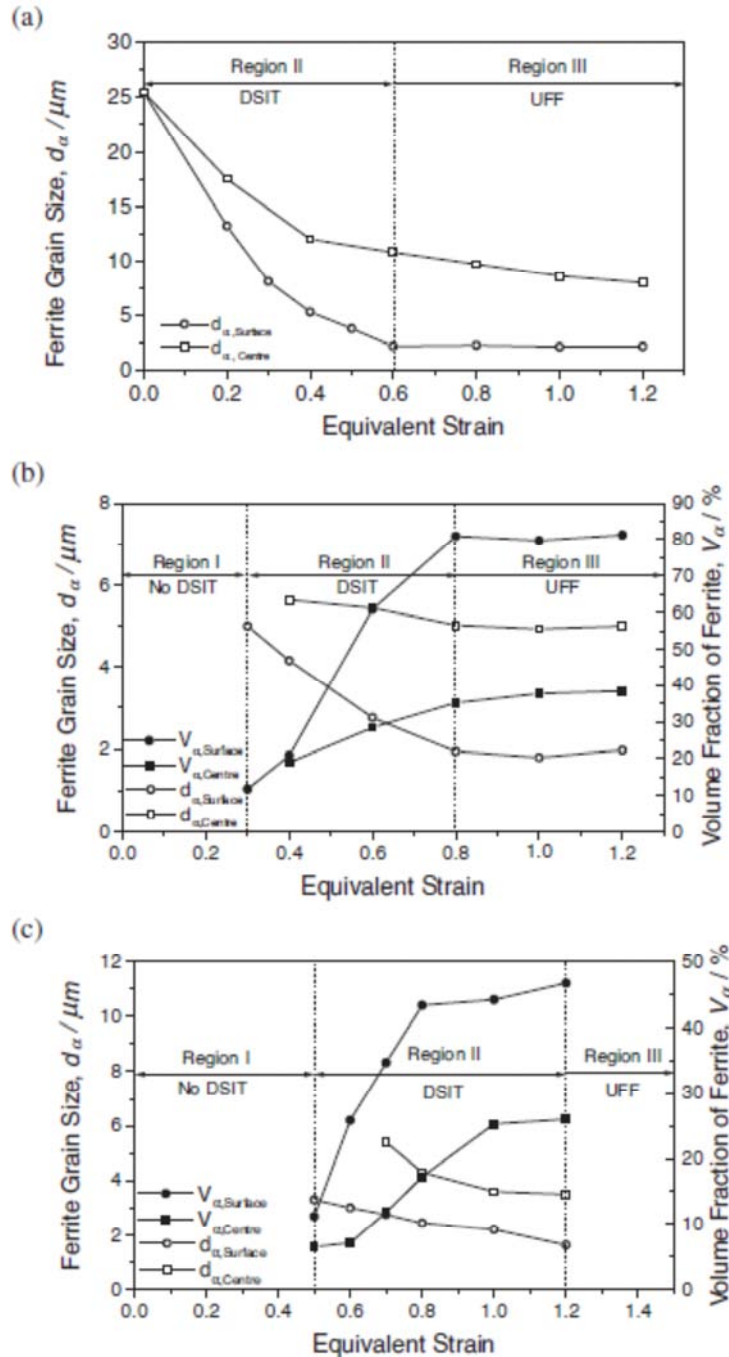


Fig. 3 Ferrite grain size and volume fraction of ferrite as a function of equivalent strain in plain carbon čeliks through single-pass rolling: (a) čelik A, (b) čelik B and (c) čelik C.

Slika 3. Veličina ferinog zrna i zapreminski udeo kao funkcija ekvivalentne deformacije na običnim ugljeničnim čelicima valjanim u jednom prolazu, (a) čelik A, (b) čelik B and (c) čelik C.



Steel	%C	$\epsilon_{C,DSIT}$	$\epsilon_{C,UFF}$
A	0.06	-----	0.6
B	0.16	0.3	0.8
C	0.35	0.5	1.2

Table 2 The critical strains for DSIT and UFF formation.
Tabela 2. Kritične deformacije za DSIT i stvaranje UFF

3. Results

The final thickness of the deformed strips was typically in the range from 2 to 2.7 mm. The microstructures of all rolled samples were inhomogeneous through the strip thickness. In addition, the ferrite transformation characteristics in the surface layer varied not only with the strain, but also with the čelik composition (carbon content). Based on this observation, the ferrite transformation characteristics could be classified into three regions as a function of strain in the surface layer (Fig. 3).

At regions that underwent low reductions, the microstructure near the surface was indistinguishable from that at the centre of the plate; only a few polygonal ferrite grains (less than 0.1 volume fraction of microstructure) formed on prior austenite grain boundaries, the rest of the microstructure being a mixture of non-polygonal ferrite (Widmansta'tten and acicular) and pearlite (hereafter called region I, Fig. 4a). The result suggested that the required strain was not sufficient for dynamic strain-induced transformation to produce polygonal ferrite grains. This region was extended to higher strains with increasing in carbon content and was not present in čelik A with the low carbon content (Fig. 3).

For locations corresponding to region II, the volume fraction of polygonal ferrite significantly increased throughout the thickness with an increase in the strain for all čeliks (Fig. 3). The ferrite grain size was significantly refined in the surface layer, although some acicular ferrite was still present in the microstructure (Figs. 3 and 4b). There were also some carbide particles on ferrite grain boundaries. The volume fraction of carbide increased with an increase in the strain and carbon content. These carbides were also arranged in elongated and narrow bands for čeliks B and C; their orientation did not appear to have any specific relationship with the rolling direction (indicated by the arrow in Fig. 4b).

3. Rezultati

Konačna debljina deformisanih traka je tipično u opsegu od 2 do 2.7 mm. Mikrostrukture svih valjanih uzoraka su nehomogene po debljini trake. Pored toga, karakteristike feritne transformacije u površinskom sloju variraju ne samo sa deformacijom, već i sa sastavom čelika (sadržaj ugljenika). Na osnovu ovog zapažanja, karakteristike feritne transformacije mogu se svrstati u tri oblasti kao funkcija deformacije u površinskom sloju (slika 3).

U oblastima gde je bilo malo sažimanje, mikrostruktura blizu površine nije se mogla razlikovati od one u centru ploče; samo nekoliko poligonalnih feritnih zrna (manje od 0,1 zapreminskog udela mikrostrukture) formiranih na granicama prethodnih austenitnih zrna, ostatak mikrostrukture je mešavina ne-poligonalnog ferita (Vidmanstašetenov i acikularni) i perlita (u daljnjem tekstu: oblast I, Slika 4a). Rezultat je sugerisao da zahtevana deformacija nije dovoljna za dinamičku transformaciju izazvanu deformacijom da bi se proizvela poligonalna feritna zrna. Ova oblast je proširena na veće deformacije sa povećanjem sadržaja ugljenika i nije bila prisutna u čeliku A sa niskim sadržajem ugljenika (slika 3).

Za lokacije koje odgovaraju oblasti II, zapreminski udeo poligonalnog ferita značajno se povećao po debljini sa povećanjem deformacije za sve čelike (Sl. 3). Veličina feritnog zrna je značajno rafinisana u površinskom sloju, mada je poneki acikularni ferit i dalje prisutan u mikrostrukтури (slike 3 i 4b). Bilo je i nešto čestica karbida na granicama feritnih zrna. Zapreminski udeo karbida se povećao sa povećanjem deformacije i sadržaja ugljenika. Ovi karbidi su takođe raspoređeni u izduženim i uskim trakama za čelike B i C; izgleda da njihova orijentacija nije imala nikakvu posebnu vezu sa pravcem valjanja (označen strelicom na slici 4b)

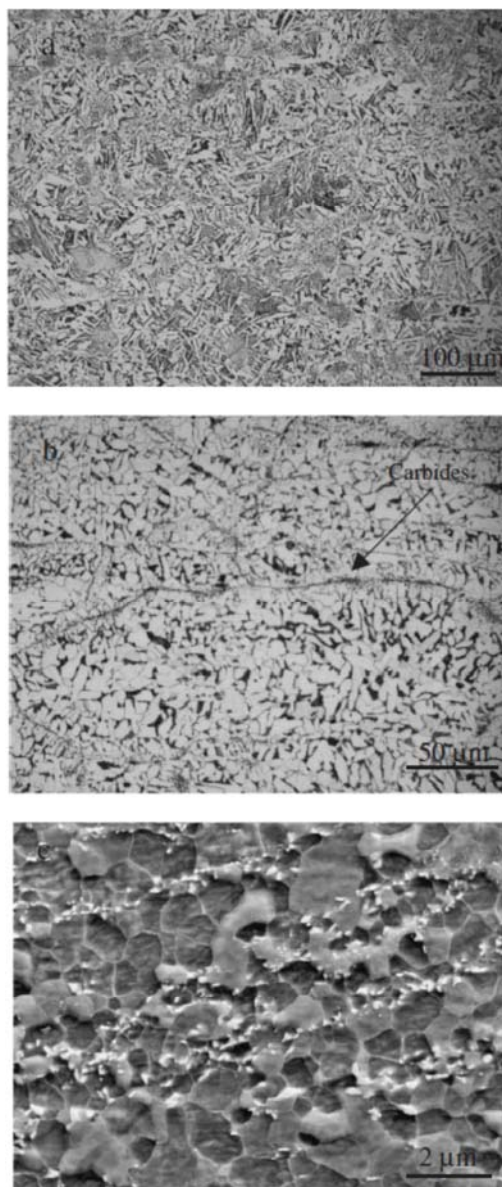


Fig. 4 The surface microstructure of steel B at different equivalent strains: a) 0, (b) 0.6 and (c) 0.8.
Slika 4. Površinska mikrostruktura čelika B pri različitim deformacijama (a) 0, (b) 0.6 and (c) 0.8.

As-quenched microstructures in region II consisted of polygonal ferrite grains mainly decorating prior austenite grain boundaries and intragranularly nucleated. This suggests dynamic strain-induced transformation of ferrite occurred during deformation. This region was also extended with an increase in the carbon content (Fig. 3).

Beyond a critical strain condition, the volume fraction of ferrite and the ferrite grain size of the surface layer did not change significantly with an increase in the strain for all čeliks (region III in Fig.3). The microstructures consisted of fully polygonal ferrite grains, as small as 1–2 μm in size, with carbide particles on ferrite grain boundary (there were also very fine pearlite and carbide bands for čeliks B and C, Fig. 4c). However, this strain was significantly increased with an increase

Mikrostrukture gašenja u oblasti II sastojale su se od poligonalnih feritnih zrna koja uglavnom dekorišu granice prethodnih austenitnih zrna i nastaju međugranulano. Ovo sugeriše dinamičku transformaciju izazvanu deformacijom ferita koji se pojavio tokom deformacije. Ova oblast se takođe širi sa povećanjem sadržaja ugljenika (slika 3).

Izvan kritičnog deformacionog stanja, zapreminski udeo ferita i veličina zrna ferita u površinskom sloju nisu se značajno promenili sa povećanjem deformacije za sve čelike (oblast III na slici 3). Mikrostrukture su se sastojale od poligonalnih feritnih zrna veličine od 1 do 2 μm , sa česticama karbida na granici feritnih zrna (bilo je i vrlo finih perlitnih i karbidnih traka kod čelika B i C, slika 4c). Međutim, ova deformacija se značajno povećava sa povećanjem sadržaja ugljenika. Površinski sloj



in carbon content. The UFF surface layer generally penetrated to about 1/4 of the total thickness.

The required strain for transition from one region to another one in the surface layer was described as a critical strain in this study. Hence, there were two critical strains; dynamic strain-induced transformation ($\epsilon_{C,DSIT}$) and ultrafine ferrite formation ($\epsilon_{C,UFF}$). These strains are summarized in Table 2 for all steels. The critical strain for both transitions increased significantly with an increase in carbon content.

In the centre of rolled strip, the microstructures were conventional ferrite and pearlite (or carbide in čelik A). The ferrite grain size decreased with an increase in the strain for all čeliks (Fig. 3). However, the change in grain size with increasing nominal strain was much lower in the centre than the surface. This is because the amount of undercooling and strain is different at the surface compared with the centre of strip. For example, at the location corresponding to an equivalent strain of 1.2, the undercooling at the surface and the centre was about 120 and 80 °C, respectively (Fig. 5).

Furthermore, it has been shown that the strain at the surface is more than three times that at the centre of strip through finite element modeling of strip rolling under heavy shear.⁷⁾ In addition, the ferrite grain size decreased with an increase in the carbon content at a given strain (Fig. 3).

UFF-a je generalno prodro na oko 1/4 ukupne debljine.

Potrebna deformacija za prelazak iz jednog područja u drugo u površinskom sloju, opisana je kao kritična deformacija u ovoj studiji. Dakle, postojale su dve kritične deformacije; dinamička transformacija izazvana deformacijom ($\epsilon_{C,DSIT}$) i formiranje ultrafinozrnog ferita ($\epsilon_{C,UFF}$). Ove deformacije su zbirno date u tabeli 2 za sve čelike. Kritična deformacija za oba prelaza značajno se povećava sa povećanjem sadržaja ugljenika.

U centru valjane trake, mikrostrukture su konvencionalni ferit i perlit (ili karbid u čeliku A). Veličina zrna ferita je smanjena sa povećanjem deformacije kod svih čelika (Sl. 3). Međutim, promena veličine zrna sa povećanjem nominalne deformacije bila je mnogo manja u centru, nego na površini. To je zato što je udeo pothlađivanja i deformacije, različit na površini u poređenju sa centrom trake. Na primer, na lokaciji koja odgovara ekvivalentnoj deformaciji od 1,2, podhlađenje na površini i centru je bilo oko 120 i 80 °C, (slika 5).

Nadalje, pokazano je da je deformacija na površini više od tri puta veća nego u središtu trake kroz modeliranje konačnim elementima, valjanja traka sa jakim smicanjem.⁷⁾ Dodatno, veličina feritnog zrna opada sa sadržajem ugljenika za datu deformaciju. (Slika 3).

T_{def} (°C)	Initial thickness of 8 mm		Initial thickness of 2 mm	
	T_s (°C)*	ΔT (°C)	T_s (°C)*	ΔT (°C)
875 ± 5	739	136	697	178
840 ± 5	713	127	669	171
790 ± 5	668	122	625	165

*The surface temperature

Table 3. The surface temperature of rolled strip at the exit point of rolls at different initial thicknesses.

Tabela 3. Temperatura površine valjane trake u tački izlaza iz valjaka sa različitim početnim debljinama

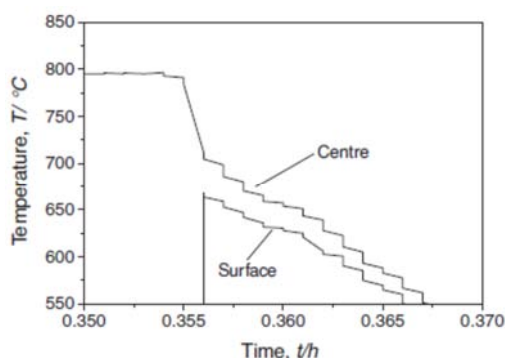


Fig. 5 Cooling curve of centre and surface of a location corresponding to plate thickness of 8mm during thermomechanical processing

Slika 5 Kriva hlađenja centra i površine na mestima koja odgovaraju debljini lima od 8 mm tokom termomehaničke obrade



4. Discussion

The single-pass rolling and subsequent air cooling of the wedge samples showed a number of important microstructural features as a function of strain which could be classified into three regions. However, the extent of regions varied significantly with the carbon content.

Region I: no dynamic strain-induced transformation

It is well known that the formation of non polygonal phases is promoted with increasing cooling rate⁸⁾ and carbon content.⁹⁾ The latter is confirmed by this study since the volume fraction of non polygonal ferrite decreased with a decrease in carbon content at a given condition (steel A is fully polygonal ferrite even at the strain free condition).

There is an increasing tendency for ferrite to grow from grain boundaries as plates (Widmanstätten morphology) with increasing cooling rate. The rapid cooling is occurred by conduction of the cold rolls in the surface of strip in singlepass rolling; the surface temperature drops about 120–180^oC during rolling depending on the initial thickness and deformation temperature (Table 3). At regions that underwent low reductions, this rapid cooling decreases the temperature to such an extent (i.e. TW; the critical temperature for Widmanstätten ferrite formation⁸⁾) that non polygonal products are promoted after straining. The result suggests that the strain was not sufficient to form the polygonal ferrite rather than non polygonal phase by DSIT in this region.

Region II: dynamic strain-induced transformation

The DSIT ferrite initially nucleates on the prior austenite grain boundary.¹⁰⁾ Therefore, the nucleation of DSIT ferrite at an early stage of transformation retards the formation of austenite grain boundary nucleated non polygonal ferrite phases (i.e. Widmanstätten ferrite) after deformation. Beyond $\epsilon_{DSIT}^{\text{C}}$, the volume fraction of ferrite nucleation sites is increased and extends from the prior austenite grain boundaries into the austenite grain interior with increase in the strain (intragranular nucleation sites). This promotes the volume fraction of polygonal ferrite grains.

It is well known that the DSIT process significantly controls the coarsening of ferrite grains during post deformation cooling.¹¹⁾ This leads to much more effective ferrite grain refinement through DSIT than conventional controlled rolling. However, the amount of coarsening depends on the volume fraction of DSIT ferrite and its distribution at an early stage of transformation. The volume fraction

4. Diskusija

Valjanje u jednom prolazu i naknadno hlađenje uzoraka klina pokazali su brojne značajne mikrostrukturne osobine kao funkciju deformacije koja se može svrstati u tri oblasti. Međutim, prostiranje oblasti značajno variraju sa sadržajem ugljenika.

Oblast I: bez transformacije izazvane dinamičkom deformacijom

Dobro je poznato da se formiranje nepoligonalnih faza bolje odvija sa povećanjem brzine hlađenja⁸⁾ i sadržaja ugljenika.⁹⁾ Ovo poslednje je potvrđeno ovom studijom jer se zapreminski udeo nepoligonalnog ferita smanjio sa smanjenjem sadržaja ugljenika u datom stanju (čelik A je u potpunosti sa poligonalnim feritom čak i u stanju bez deformacije).

Postoji sve veća tendencija da ferit raste sa granica zrna kao ploče (Widmanštetenova morfologija) sa povećanjem brzine hlađenja. Brzo hlađenje nastaje provođenjem hladnih valjaka po površini trake u jednostrukom valjanju; temperatura površine pada za oko 120-180 °C tokom valjanja u zavisnosti od početne debljine i deformacione temperature (Tabela 3). U područjima koja su podvrgnuta malim sažimanjima, ovo brzo hlađenje smanjuje temperaturu do te mere (tj. TW; kritična temperatura za stvaranje Vidmanštetenovog ferita⁸⁾) da se nepoligonalni proizvodi ne javljaju posle deformacije. Rezultat sugerše da deformacija nije bila dovoljna da stvori poligonalni ferit, već više nepoligonalnu fazu DSIT-om u ovoj oblasti.

Oblast II: transformacija izazvana dinamičkom deformacijom .

DSIT ferit se u početku stvara na granici prethodnog zrna austenita.¹⁰⁾ Zbog toga, nastajanje DSIT ferita u ranoj fazi transformacije usporava formiranje nepoligonalne feritne faze na granicama austenitnog zrna (tj. Vidmanštetenov ferit) nakon deformacije. Iza $\epsilon_{DSIT}^{\text{C}}$, povećava se zapreminski udeo mesta nastajanja ferita i proteže se od granica prethodnih austenitnih zrna u unutrašnjost austenitnog zrna sa povećanjem deformacije (intragranularna mesta nastajanja). To pogoduje zapreminskom udelu poligonalnih feritnih zrna.

Dobro je poznato da DSIT proces značajno kontroliše ogrubljenje feritnih zrna tokom postdeformacionog hlađenja.¹¹⁾ To dovodi do mnogo efikasnije rafinacije feritnih zrna kroz DSIT od konvencionalnog kontrolisanog valjanja. Međutim, količina ogrublosti zavisi od zapreminskog udela DSIT ferita i njegove raspodele u ranoj fazi transformacije. Zapreminski



of DSIT ferrite grains increases with an increase in the strain (i.e. increasing the Ar3 temperature) at the early stage of transformation in region II. This increases the impingement of DSIT ferrite grains as a function of the strain at the early stage of transformation, which thereby controls the coarsening of ferrite grains during post deformation cooling.¹¹⁾ This promotes the ferrite grain refinement with an increase in the strain in region II.

Region III: ultrafine ferrite formation

Beyond a given condition, the volume fraction of polygonal ferrite and ferrite grain size of the surface layer do not change significantly for all čeliks. The resultant ferrite grain size is as small as 1–2 μm . Indeed, the coarsening rate is independent of strain in region III. This suggests that the volume fraction of DSIT ferrite and its distribution at the early stage of transformation does not alter significantly beyond $\epsilon_{C, UFF}$. This leads to a constant final ferrite grain size in this region. Although the current work confirms that UFF formation is independent of čelik composition, the critical strains for DSIT ferrite and UFF formation are significantly altered by carbon content. It is proposed that the effect of carbon content in postponing the critical strains for DSIT and UFF formation could be explained by the stacking fault energy (SFE) value, the prior austenite grain size and the chemical driving force for dynamic ferrite transformation. Although, the SFE parameter has been shown to have a strong influence on the behaviour of metals and alloys during deformation,¹²⁾ Charnock et al.¹³⁾ proved the carbon content (0.005–0.83% mass C) does not have a significant effect on the SFE. It is well established that the number of intragranular defects formed during deformation is raised by increasing the austenite grain size.¹⁴⁾ A recent study¹⁰⁾ has shown that the $\epsilon_{C, DSIT}$ significantly decreased (from 0.5 to 0.1) with an increase in the prior austenite grain size (from 14 to 80 μm), this had a slight change on $\epsilon_{C, UFF}$. Since the prior austenite grain size is higher than 120 μm in this study, it is unlikely the prior austenite grain size could have a significant influence on these critical strains. During dynamic strain-induced transformation of austenite to ferrite, the driving force for nucleation and growth of ferrite in the austenite region comes from the deformation (i.e. reduction) and the composition. Decreasing the carbon content increases the equilibrium transformation temperature and the Ar3 for low carbon steels. Hence, for a given state of the austenite, it would be expected that transformation of ferrite will occur at a higher temperature and faster rate for a lower carbon content. A simple explanation for DSIT is that the

udeo DSIT feritnih zrna se povećava sa povećanjem deformacije (tj. povećanjem temperature Ar3) u ranoj fazi transformacije u oblasti II. Ovo povećava učestalost DSIT feritnih zrna kao funkciju deformacije u ranoj fazi transformacije, koja time kontroliše ogrubljenje feritnih zrna tokom naknadnog deformacionog hlađenja.¹¹⁾ Ovo doprinosi rafinaciji feritnog zrna sa povećanjem deformacije u oblasti II.

Oblast III: formiranje ultrafinozrnog ferita

Izvan datog stanja, zapreminski udeo poligonalnog ferita i veličine feritnog zrna u površinskom sloju ne menja se značajno za sve čelike. Dobijena veličina zrna ferita je samo 1–2 μm . Zaista, brzina ogrubljenja je nezavisna od deformacije u oblasti III. To sugeriše da se zapreminski udeo DSIT ferita i njegova raspodela u ranoj fazi transformacije ne menjaju značajno iznad $\epsilon_{C, UFF}$. To dovodi do konstantne konačne veličine zrna ferita u ovoj oblasti.

Iako sadašnji rad potvrđuje da je formiranje UFF-a nezavisno od sastava čelika, kritične deformacije za formiranje DSIT ferita i UFF-a značajno su izmenjeni sadržajem ugljenika. Predloženo je da se efekat sadržaja ugljenika u odlaganju kritičnih deformacija za formiranje DSIT-a i UFF-a može objasniti vrednošću energije slaganja grešaka (SFE), prethodnom veličinom zrna austenita i hemijskom pokretačkom snagom za dinamičku transformaciju ferita. Iako je pokazano da parametar SFE ima jak uticaj na ponašanje metala i legura tokom deformacije,¹²⁾ Charnock i dr.¹³⁾ su dokazali da sadržaj ugljenika (0,005–0,83% mas) nema značajan uticaj na SFE. Dobro je utvrđeno da je broj intragranularnih defekata nastalih tokom deformacije povećan sa povećanjem veličine zrna austenita.¹⁴⁾ Nedavna studija¹⁰⁾ je pokazala da je $\epsilon_{C, DSIT}$ značajno smanjen (od 0.5 do 0.1) sa povećanjem veličine prethodnog zrna austenita (od 14 do 80 μm), tako da je to izazvalo malu promenu $\epsilon_{C, UFF}$. S obzirom da je veličina zrna prethodnog austenita veća od 120 μm u ovoj studiji, malo je verovatno da veličina zrna prethodnog austenita može imati značajan uticaj na ove kritične deformacije. Tokom transformacije izazvane dinamičkom deformacijom austenita u ferit, pokretačka sila za nastanak i rast ferita u oblasti austenita dolazi od deformacije (tj. redukcije-sažimanja) i sastava. Smanjenje sadržaja ugljenika povećava ravnotežnu temperaturu transformacije Ar3 kod nisko-ugljeničnih čelika. Dakle, za dato stanje austenita, moglo bi se očekivati da će se transformacija ferita odvijati pri višoj temperaturi i većoj brzini za niži sadržaj ugljenika. Jednostavno objašnjenje za DSIT je da se Ar3 povećava tokom



Ar₃ increases during deformation with increasing strain until reaches the temperature of the deformation. From this it would be expected that a higher Ar₃ before deformation will allow this condition to be met at a lower strain. Hence, it is likely that with an increase in carbon content, the reductions required for dynamic ferrite transformation and later UFF formation would be increased (i.e. nucleation and growth of ferrite). This supports the decrease in the critical strain for UFF formation in čelik A from 1.2 (for čelik C) to 0.6.

5. Conclusions

(1) There were a number of important microstructural features as a function of strain through single-pass rolling and subsequent air cooling of the wedge samples. Based on the observation, three regions were determined as follows: Region I: no dynamic strain-induced transformation Region II: dynamic strain-induced transformation Region III: ultrafine ferrite grain formation

(2) There were two critical strains for DSIT ferrite and ultrafine ferrite formation.

(3) The carbon content has shown a significant effect on these critical strains. The critical strains were postponed to a higher value with an increase in the carbon content.

(4) The effect of carbon content in postponing the critical strains for DSIT and UFF formation could be explained by the chemical driving force for dynamic ferrite transformation.

Acknowledgements

This work was supported by the Australian Research Council. The technical assistance of J. Whale and R. Pow is gratefully acknowledge. H. Beladi also acknowledges the support of a Deakin University research scholarship.

References

Literatura

- 1) R. Priestner: Thermomechanical Processing of Microalloyed Austenite, ed. by A. J. DeArdo, G. A. Ratz and P. J. Wray, (TMS-AIME, Warrendale, PA, 1981) 455–466.
- 2) J. H. Beynon, R. Gloss and P. D. Hodgson: Mater. Forum 16 (1992) 37–42.
- 3) P. D. Hodgson, M. R. Hickson and R. K. Gibbs: Scr. Mater. 40 (1999) 1179–1184.
- 4) M. R. Hickson, R. K. Gibbs and P. D. Hodgson: ISIJ Int. 39 (1999) 1176–1180.
- 5) H. Yada, C. M. Li and H. Yamagata: ISIJ Int. 40 (2000) 200–206.
- 6) R. Priestner, Y. M. Al-Horr and A. K. Ibraheem: Mater. Sci. Technol. 18 (2002) 973–980.
- 7) X. J. Zhang, P. D. Hodgson and P. F. Thomson: Mater. Process. Technol. 60 (1996) 615–619.

deformacije sa povećanjem deformacije dok ne dostigne temperaturu deformacije. Iz ovoga se može očekivati da će veći Ar₃ pre deformacije omogućiti da se ovo stanje zadovolji pri manjoj deformaciji. Prema tome, verovatno je da će se sa povećanjem sadržaja ugljenika povećati potrebno sažimanje za dinamičku transformaciju ferita i kasnije formiranje UFF-a (tj. nastajanje i rast ferita). Ovo podržava smanjenje kritične deformacije za formiranje UFF-a u čeliku A sa 1,2 (za čelik C) na 0,6.

5. Zaključci

(1) Postojala su brojna značajna mikrostrukturalna svojstva kao funkcija deformacije kroz jednostepeno valjanje i naknadno hlađenje na vazduhu uzoraka klina. Na osnovu posmatranja, tri oblasti su određene na sledeći način:

Oblast I: nema dinamičke transformacije izazvane deformacijom Oblast II: dinamička transformacija izazvana deformacijom Oblast III: formiranje ultrafinozrnog ferita

(2) Postojala su dve kritične deformacije za DSIT ferit i formiranje ultrafinozrnog ferita.

(3) Sadržaj ugljenika je pokazao značajan uticaj na ove kritične deformacije. Kritične deformacije su pomerene na veću vrednost s povećanjem sadržaja ugljenika.

(4) Uticaj sadržaja ugljenika u odlaganju kritičnih deformacija za formiranje DSIT-a i UFF-a mogao bi se objasniti hemijskom pokretačkom snagom za dinamičku transformaciju ferita.

Zahvalnost

Ovaj rad je podržan od strane Australian Research Council. Na tehničkoj pomoći J. Vhale-a i R. Pov-a smo veoma zahvalni. H. Beladi takođe zahvaljuje na podršci za stipendiju Deakin univerziteta

- 8) D. A. Porter and K. E. Easterling: Phase Transformations in Metals and Alloys, (2nd ed., London, Chapman & Hall, 1992).
- 9) R. F. Mehl and C. A. Dube: Phase Transformations in Solids, (John Wiley, New York, 1951).
- 10) H. Beladi, G. L. Kelly, A. Shokouhi and P. D. Hodgson: Mater. Sci. Eng. A 367 (2004) 152–161.
- 11) H. Beladi, A. Zarei-Hanzaki, G. L. Kelly and P. D. Hodgson: Mater. Sci. Technol. 20 (2004) 213–220.
- 12) B. Bay, N. Hansen, D. A. Hughes and D. Kuhlmann-Wilsdorf: Acta Metall. Mater. 40 (1992) 205–219.
- 13) W. Charnock and J. Nutting: Metal Sci. J. 1 (1967) 123–127.
- 14) R. Bengochea, B. Lopez and I. Gutierrez: ISIJ Int. 39 (1999) 583–591



Republičko takmičenje mladih zavarivača
„Mladi zavarivač 2019“, Novi Sad, 10-11. Maj 2019

Nastavak sa strane 52.

Fotografije sa takmičenja

REL (111)



MAG (135)





TIG (141)



Komisija DUZS za ocenjivanje uzoraka



Najuspešniji takmičari po postupcima:

Postupak 111 – REL		
Učenik	Mentor	Škola
1. Tomić Dejan	Gajić Ivan	Tehnička škola „Kolubara“ Lazarevac
2. Nikolić Nemanja	Vilotić Radoslav	Tehnička škola Obrenovac
3. Jankulović Slobodan	Vlaisavljević Nikola	Srednja tehnička škola “Milenko Brzak Uča“, Ruma
Postupak 135 – MAG		
Učenik	Mentor	Škola
1. Simunović Aleksandar	Gajić Ivan	Tehnička škola „Kolubara“ Lazarevac
2. Živković Marko	Lukić Zoran	Tehnička škola Obrenovac
3. Lukač Bojan	Jankov Aleksandar	Srednja mašinska škola Novi Sad,
Postupak 141 – TIG		
Učenik	Mentor	Škola
1. Mladenović Željko	Antić Igor	Mašinska škola Niš
2. Sklenar Roland	Husar Čila	Tehnička škola “Ivan Sarić“ Subotica
3. Filipović Nemanja	Vasiljević Milovan	Srednja škola “17.septembar“ Lajkovac



Rang lista ekipno:

R. br.	NAZIV ŠKOLE	MESTO	Mentor
1	Tehnička škola „Kolubara“	Lazarevac	Gajić Ivan
2	Tehnička škola	Obrenovac	Bilotić Radoslav
3	Srednja tehnička škola “Milenko Brzak Uča“	Ruma	Vlaisavljević Nikola
4	Tehnička škola	Vlasotince	Miljković Srboljub
5	Tehnička škola „Ivan Sarić“	Subotica	Husar Čila
6	Srednja škola“17.septembar“	Lajkovac	Vasiljević Milovan
7	Tehnička škola	Železnik	Krstić Stanoje
8	Tehnička škola	Čuprija	Stevanović Srboljub
9	Tehnička škola	Odžaci	Stamenković-Kovljančić Slađana
10	Mašinska škola	Niš	Nenić Dragana
11	Srednja mašinska škola	Novi Sad	Jankov Aleksandar
12	Tehnička škola	Kosovska Kamenica	Jordanović Zoran
13	Srednja stručna škola	Kragujevac	Lazin Jasmina
14	Srednja škola	Krupanj	Novičić Zoran
15	Prva tehnička škola	Kruševac	Gavrilović Zoran
16	Tehnička škola sa domom učenika “Nikola Tesla“	Kostolac	Petković Stojanča

Najuspešnijim takmičarima podeljene su i vredne nagrade



ČASOPIS ZAVARIVANJE I ZAVARENE KONSTRUKCIJE**Cenovnik oglasnog prostora u četiri uzastopna broja 2019**

	A4	2/2	1/1	1/2	1/4	1/8
dimenzije (mm)		2 x 210 x 297	210 x 297	180 x 120	90 x 120	90 x 60
DIN	crno/beli	-	39 000	23 000	16 000	10 000
	kolor	105 000	75 000	-	-	-

- U cene nije uračunat PDV 20%.
- Objavljivanje oglasa u samo jednom broju iznosi 30% od datih cena.
- Reklamni tekstovi: 25 % od cene površine crno/belih oglasa.
- Dostava materijala:
 - za crno-beli film ili CD (Adobe Photoshop / CorelDRAW);
 - za kolor film ili CD (Adobe Photoshop / CorelDRAW);
 - izrada filma sa CD: 10 % od cene angažovanog prostora.
- Na web prezentaciji DUZS-a, (www.duzs.org.rs), na strani Marketing, objavljuje se pregled firmi-oglašivača sa podacima o glavnim grupama proizvoda/usluga i adresom web prezentacije. Svi posetioci naše web prezentacije mogu da posete i web prezentacije oglašivača, preko aktivnih linkova koji se nalaze na ovoj stranici!

WELDING & WELDED STRUCTURES, Quarterly review
Advertising prices for four successive numbers in 2019

	A4	2/2	1/1	1/2	1/4	1/8
dimensions (mm)		2 x 210 x 297	210 x 297	180 x 120	90 x 120	90 x 60
EUR	black/white	-	840	432	336	240
	colour	2 640	1 680	-	-	-

- VAT 20% included.
- Advertising in one number only is 35% of the given prices.
- Commercial articles: 30 % of black/white advertising price.
- Print material:
 - for black/white CD (Adobe Photoshop / CorelDRAW)
 - for color CD (Adobe Photoshop / CorelDRAW).
- All the visitors of our web site may be linked to the advertisers' web site.

INDEKS OGLAŠIVAČA
ADVERTISERS INDEX

DUCTIL SA
 WELD-ING
 YASKAWA SLOVENIJA
 HONEX
 ELIMP
 NEMINIK
 MESSER TEHNOGAS
 APAVE Ver Tech Serbia

1. ČLANARINA DUZS za 2019. godinu **3.500 dinara**
 Članovima DUZS **GRATIS** godišnje izdanje časopisa "ZAVARIVANJE I ZAVARENE KONSTRUKCIJE"
2. ČASOPIS "ZAVARIVANJE I ZAVARENE KONSTRUKCIJE" - 2019. godina
 u slobodnoj prodaji (u cene je uračunat PDV 10%):
 - cena pojedinačnog broja..... 825 dinara
 - godišnja pretplata za 1 komplet brojeva godišnjeg izdanja..... 2.500 dinara
3. ČASOPIS - stari brojevi (u cene je uračunat PDV 10%)
 - a) u slobodnoj prodaji:
 - cena pojedinačnog broja za 2017. godinu 500 dinara
 - cena pojedinačnog broja za prethodne godine..... 250 dinara
 - b) beneficirane cene za članove DUZS:
 - cena pojedinačnog broja za 2018. godinu (pouzećem ili preuzimanjem) 400 dinara
 - cena pojedinačnog broja za prethodne godine (pouzećem ili preuzimanjem) Gratis
4. Knjiga Organizacija i ekonomika zavarivačkih radova – autor: prof. dr Zoran Radojević (uračunat PDV 10%) 1.045 dinara
5. Zbirke standarda OBEZBEĐENJE KVALITETA U ZAVARIVANJU, komplet 4 toma 6.750 dinara